ARDHI UNIVERSITY

COMPARISON OF WATER VAPOUR COMPUTED FROM GNSS AND GLOBAL WEATHER MODEL FOR NUMERIC WEATHER PREDICTION IN TANZANIA

KODI, SALMA R

BSc Geomatics

Dissertation

Ardhi University, Dar es Salaam

July, 2023

COMPARISON OF WATER VAPOUR COMPUTED FROM GNSS AND GLOBAL WEATHER MODEL FOR NUMERIC WEATHER PREDICTION IN TANZANIA

BY KODI SALMA

A Dissertation Submitted to the Department of Geospatial Sciences and Technology in Partial Fulfilment of the Requirements for the Award of Bachelor of Science in Geomatics (BSc. GM) of Ardhi University

CERTIFICATION

The undersigned certify that they have read and hereby recommend for acceptance by the Ardhi University a dissertation titled **"Comparison of Computed Water Vapour from GNSS and Global Weather Model for Numerical Weather Prediction in Tanzania"** in partial fulfillment of the requirements for the award of degree of Bachelor of Science in Geomatics at Ardhi University.

Signature…… **Signature…….**

Dr. Elifuraha Saria
(Main Supervisor)
Date……...

Ms. Valerie Ayubu
(Second Supervisor)
Date……

DECLARATION AND COPYRIGHT

I, KODI SALMA hereby declare that, the contents of this dissertation are the results of my own findings through my study and investigation, and to the best of my knowledge they have not been presented anywhere else as a dissertation for diploma, degree or any similar academic award in any institution of higher learning.

……..

KODI SALMA R

22822/T.2019

(Candidate)

ACKNOWLEDGEMENT

First of all, I would humbly like to thank Lord, the Almighty for taking me this far and for sure; he didn't bring me this far to abandon me.

I would like to express my appreciation to Dr. Elifuraha Saria who inspired me towards this study and Ms. Valerie Ayubu for their memorable and valuable supervision towards accomplishment of this Dissertation. I would also like to thank all academic staff of Department of Geospatial Sciences and Technology (DGST) for their guidance in four years at Ardhi University.

I would also like to express my gratitude towards my fellow colleagues Kiluswa Johnson, Masatu Masatu, Sylvanus Daniel, Abdallah Machemba, Edgar Mlawa, Happiness Swai, Harry Chove and Peter Mathias together with all Geomatics and Geoinformatics classmates for their love and support. I value their steadfast cooperation, contribution and willingness to offer trustworthy support whenever I needed it.

My special thanks go toward Mr. Timotheo Joseph for being by my side towards this achievement, may your life cherish with sweet fruits.

Last but not least, I would like to happily thank my lovely family; my lovely father Mr. Rajab Othman Kodi, my lovely mother Ms. Aisha Rajab and my lovely sister Sada. May God protect you, always.

DEDICATION

I sincerely dedicate this dissertation to myself and my lovely young sister, Sada Rajab for the battles she has been fighting, pain endured, failures faced and the victory she is to achieve. I hope she knows we will win together with the help of Allah.

ABSTRACT

Global Navigational Satellite System (GNSS) over the past and present time has shown a great potential in the retrieval of the distribution of water vapour in the atmosphere. Taking the advantage of the effect of the atmosphere on GNSS signal as they travel from the constellation of satellite to ground-based GNSS receivers much information (water vapour content) about the atmosphere (mostly from the troposphere) can be derived is referred to as GNSS meteorology. The ionosphere and the troposphere are among the major causes of GNSS signal delay as they travel down to the earth surface from the constellation of satellites. The ionospheric delay can be mitigated using dual frequency GNSS receivers and utilizing its dispersive characteristics. This research presents the spatiotemporal variability of Precipitable Water Vapour (PWV) retrieved from ground–based Global Navigation Satellite System (GNSS) stations over Tanzania for the years 2015.

In this research, the GNSS data were processed using GAMIT/GLOBK software. Data processing by this GNSS software involved creating the working directories where the data inputted in the software were kept, creating tables, updating site information on station.info file, running sh_gamit command and running utility sh_metutil. The output contained the atmospheric values whereby time, PW estimates and their sigma were of interest. The PWV values estimated from GAMIT/GLOBK GNSS software were then grouped into daily and monthly averages; the variability of the daily and monthly GNSS PWV were compared and validated with the daily and monthly PWV from the Global Reanalysis Data Era-interim. The results revealed that the spatiotemporal variability of PWV across Tanzania is a function of geographic location and seasons. Also, it shows that there is a positive correlation between GNSS PWV and Global Reanalysis Data PWV of ARSH, DODM and MTVE which are 0.81859, 0.92434 and 0.89186 respectively. The research also affirms that GNSS PWV could be used to improve weather forecasting/monitoring as well as climate monitoring.

Keywords: Global Navigation Satellite System Precipitable Water Vapour (GNSS PWV), Global Reanalysis Data Era-Interim.

TABLE OF CONTENT

CERTIFICATION ii
DECLARATION AND COPYRIGHT iii
ACKNOWLEDGEMENT iv
DEDICATION v
ABSTRACT vi
LIST OF FIGURES x
ACRONYMS AND ABBREVIATIONS xii
CHAPTER ONE 1
INTRODUCTION 1
1.1 Background of the problem 1
1.2 Related Studies 3
1.3 statement of the research problem 4
1.4 Objectives of the Research 4
1.4.1 Main Objectives 4
1.4.2 Specific objectives 4
1.5 Study Area 5
1.6 Significance and beneficiaries of the research 5
1.7 Limitation of the Research 6
1.8 Organization of the research 6
CHAPTER TWO 7
LITERATURE REVIEW 7
2.1 Meteorology 7
2.1.1 Atmosphere 7
2.1.2 Weather and Climate 8
2.1.3 Weather forecasting 8
2.1.4 Reanalysis Data 10
2.2 Tanzania Meteorological Agency (TMA) 12
2.2.1 Meteorological Observation Techniques 13
2.2.2 Numerical Weather Prediction 14
2.3 Water Vapour 15
2.3.1 Water vapour measurement techniques 15
2.4 GNSS 16

2.4.1 Meteorological GNSS Observation 17
2.5 Time Series Analysis 17
2.6 Correlation Analysis 17
2.7 Related Studies 19
CHAPTER THREE 20
METHODOLOGY 20
3.1 Data Identification 20
3.2 Data Source and Acquisition 21
3.2.1 RINEX observation, meteorological, navigation files for experiment sites and RINEX observation files for IGS sites. 21
3.2.2 Integrated water vapor (IWV) from Global reanalysis data 21
3.2.3 Precise ephemeris and precise clock files 22
3.4 Data Format 22
3.4.1 RINEX observation files for experiment and IGS sites. 22
3.4.2 RINEX meteorological file 23
3.4.3 IWV from Global reanalysis data (ERA-Interim) 23
3.5 Data Processing 23
3.5.1 Creating working directory 23
3.5.2 Creation of tables 24
3.5.3 Updating site information on statio.info file 24
3.5.4 Running sh_gamit to get O-files 24
3.5.5 Running the utility sh_metutil 26
3.6 Analysis on computed PW/IWVs 26
CHAPTER FOUR 27
RESULTS AND ANALYSIS 27
4.1 GNSS Precipitable Water Vapour 27
4.1.1 Time series analysis of the computed Precipitable Water Vapour 27
4.1.2 Descriptive analysis of the computed PW 28
4.2 The IWV from global Reanalysis data of ERA-Interim 28
4.2.1 Time series analysis on PW of Era-interim 28
4.2.2 The descriptive analysis of $PW_{ERA\text{-}Interim}$ 30
4.3 The comparison between Global Reanalysis data and GNSS computed PW for ARSH Cors Station. 31

4.3.1 Time series analysis of PW of Era-interim and PW computed from GAMIT/GLOBK 31
4.3.2 The Descriptive Analysis of PW of ERA-Interim and PW from GAMIT/GLOBK.... 32
4.3.3 Difference between the PW from GAMIT and PW from reanalysis data Era-interim 33
4.3.4 The correlation analysis between the PW computed from GAMIT and PW from reanalysis data Era-interim 33
4.4 The comparison between Global Reanalysis data and GNSS computed PW for DODM Cors Station. 34
4.4.1 Time series analysis of PW of Era-interim and PW computed from GAMIT/GLOBK 34
4.4.2 The Descriptive Analysis of PW of ERA-Interim and PW from GAMIT/GLOBK.... 35
4.4.3 Difference between the PW from GAMIT and PW from reanalysis data Era-interim 35
4.4.4 The correlation analysis between the PW computed from GAMIT and PW from reanalysis data Era-interim 36
4.5 The comparison between Global Reanalysis data and GNSS computed PW for MTVE Cors Station. 36
4.5.1 Time series analysis of PW of Era-interim and PW computed from GAMIT/GLOBK 36
4.5.2 The Descriptive Analysis of PW of ERA-Interim and PW from GAMIT/GLOBK.... 37
4.5.3 Difference between the PW from GAMIT and PW from reanalysis data Era-interim 38
4.5.4 The correlation analysis between the PW computed from GAMIT and PW from reanalysis data Era-interim 39
4.7 Summary of the results 40
CHAPTER FIVE 41
CONCLUSION AND RECOMMENDATION 41
5.1 CONCLUSION 41
5.2 RECOMMENDATIONS 42
REFERENCES 43
APPENDICES 44

LIST OF FIGURES

Figure 1. 1 Map of Study area 5
Figure 3.1 EarthScope Consortium Data Download Center 21
Figure 3.2 Uncrinexing Hatanaka files using crx2rnx 22
Figure 3.3 Workflow for processing GNSS Data by using GAMIT Software 24
Figure 4.1 Time series showing the computed PW from GNSS Cors station 27
Figure 4.2 PWERA-interim for ARSH Cors station 29
Figure 4. 3 PWERA-interim for DODM Cors station 29
Figure 4. 4 PWERA-Interim for MTVE Cors station 30
Figure 4. 5 Comparison of PWgamit and PWERA-Interim for ARSH station 31
Figure 4. 6 Difference between PWERA-interim and PWgamit for ARSH station 33
Figure 4. 7 Correlation between the Computed PW and the PWERA-Interim for ARSH 33
Figure 4. 8 Comparison of PWgamit and PWERA-Interim for DODM station 34
Figure 4. 9 Difference between PWERA-interim and PWgamit for DODM station 35
Figure 4. 10 Correlation between the Computed PW and the PWERA-Interim for DODM 36
Figure 4. 11 Comparison of PWgamit and PWERA-Interim for MTVE station 37
Figure 4. 12 Difference between PWERA-interim and PWgamit for MTVE station 38
Figure 4. 13 Correlation between the Computed PW and the PWERA-Interim for MTVE 39

LIST OF TABLES

Table 2.1 Overview of Reanalysis models 12
Table 2.2 Weather Observation Techniques 14
Table 3.1 Data Identification for the Research 20
Table 4.1 Descriptive Analysis of the computed PW 28
Table 4. 2 Descriptive Analysis of the PW from ERA-Interim 30
Table 4. 3 Descriptive Analysis of PWERA-Interim and Computed PW for ARSH Station 32
Table 4. 4 Descriptive Analysis of PWERA-Interim and Computed PW for DODM Station 35
Table 4. 5 Descriptive Analysis of PWERA-Interim and Computed PW for MTVE Station 38
Table 4. 6 Pearson Correlation Coefficient 40
Table 4. 7 Summary of PW values in wet and dry season 40

ACRONYMS AND ABBREVIATIONS

AMDAR	Aircraft Meteorological Data Relay
CORS	Continuous Operating Reference Station
ECMWF	European Centre for Medium-Range Weather Forecasts
GFS	Global Forecast System
GUAN	Global Upper Air Network
GNSS	Global Navigation Satellite System
GPS	Global Positioning System
IPWV	Integrated Precipitable Water Vapour
LIDAR	Light Detection and Ranging
MOS	Model Output Statistics
MWRs	Microwave Radiometers
NWP	Numerical Weather Prediction
PPP	Precise Point Positioning
PROBEX	Predictability and Observation Experiment in Korea
RAOBs	Radiosondes
TMA	Tanzania Meteorological Agency
ZHD	Zenith Hydrostatic Delay
ZWD	Zenith Wet Delay
ZTD	Zenith Total Delay

CHAPTER ONE

INTRODUCTION

1.1 Background of the problem

Water vapor is the key element in the hydrological cycle and the main driver of atmospheric events. It is one of vital meteorological parameters which play an important role in Numeric Weather Prediction (NWP) which is currently the most preferred way in weather forecasting. Water vapor is not evenly distributed over the earth because of the hydrological cycle and variations of temperature, pressure and geography. The distribution varies both horizontally on earth's surface and vertically as well. Nearly 50% of the water in the atmosphere is between sea level and 1.5 km above sea level. Less than 5% is between 5 to 12 km and less than 1% is in the stratosphere. Horizontally, on earth's surface, average Integrated Precipitable Water Vapor (IPWV) is less than 5 mm near the poles and greater than 50 mm near the equator. Active weather is strongly correlated to the distribution of water vapor in the atmosphere. Measurement of atmospheric water vapor has been performed by variety of techniques including convection methods like radiosondes (RAOBs), microwave radiometers (MWRs), remote sensing satellites, and later Global Navigation system (GNSS) (Ha *et al*., 2010).

Currently, a radiosonde is the most widely used water-vapor measuring device, it is composed of a meteorological sensor which measures pressure, temperature, and humidity as the balloon soars up. About 900 World Meteorological Organization radiosonde stations, under the World Weather Watch program, launch radiosondes several times a day. Remote sensing satellites can measure water vapor at a much larger area to global scale by observing the brightness temperature of the atmosphere using onboard infrared and microwave sensors. One of the disadvantages of satellite-based measurements is that one cannot use infrared sensors to retrieve data on water vapor content under clouds and even though microwave sensors can measure water vapor even under cloud, but they only work in oceanic parts of the Earth because of their relatively simple surface condition (Zhou *et al*., 2016). Though it is the most important parameter in NWP, still measurement of atmospheric water vapor by available convection methods like radiosondes, microwave water radiometers and hygrometers are too expensive to be affordable by most of countries and organizations for example in Tanzania there are four radiosondes and also, they are affected by meteorological conditions. The existing systems for water vapor measurement are inadequate in global scale and hence there is a clear need of

developing a system that is highly accurate with high temporal and spatial resolution, free from meteorological conditions, low maintenance and most of all relatively cheaper (Wolfe & Gutman, 1999).

Global Navigation Satellite Systems (GNSS) is a term used to describe all forms of satellite-based navigation systems and encompasses all satellite radio-navigation systems that can be accessed globally and provide signals for navigation, positioning, surveillance and timing information for ground, marine, aviation and space applications (Hofmann *et al*., 2008). Different GNSS systems have been developed and some are fully operational giving highly precise positioning, navigation, time services and other various outer space applications The GNSS meteorology (before GPS meteorology) was suggested by (Bevis *et al*., 1992) and later on 1997; it was clarified more by Solheim and Ware., 1999. The concept is based on propagation delays due to neutral atmosphere as the magnitude of signal delay was treated to be proportional to the amount of water vapour in atmosphere (Bevis *et al*., 1992).The delayed GPS signals by atmosphere and ionosphere are considered as errors and not needed in geodetic applications but interestingly they become useful atmospheric parameters when well modeled (Schüler, 2001). Sensing meteorological parameters using GNSS signals can be achieved using ground-based surface network of GNSS receivers or space-borne GNSS receivers on board a low Earth orbiting (LEO) satellite (De haan, 2008).

From that possibility, different ground-based systems have been developed to provide such important parameters for meteorological applications especially in mid-latitude region, for example for Europe, in 2003 the Targeting Optimal Use of GPS Humidity measurements (TOUGH) was introduced with aim of obtaining high quality atmospheric moisture information for the forecasting network from existing network of GPS stations (Vedel, 2004). Also, Japan Meteorological Agency (JMA) has been working with Geographic Survey Institute to get integrated water vapour (IWV) products from a network of about thousands of GPS receivers which are distributed all over Japan (Ishihara, 2005).

1.2 Related Studies

Several researches on GNSS meteorology have been conducted in study about meteorological values obtained from GNSS and other systems.

A research was conducted on the comparison of PW obtained at Kwame Nkrumah University of science and Technology GPS station by Precise Point Positioning (PPP) and those from Global reanalysis data in 2017 (Acheampong *et al*., 2017). The result showed a positive correlation between them over Ghana. This is one of few researches on Atmospheric water vapour which was conducted in equatorial region and especially Africa.

The National Institute of Meteorological Research of Korea conducted PROBEX2009 (Predictability and Observation Experiment in Korea) in Ulleungdo from August 20 through September 30 and water vapour profiles for 14 days including periods of severe weather condition were estimated from MWR, GPS and RAOB. In particular, the standard deviation of wet refractivity profiles between GPS with MWR was smaller than the STD between RAOB and MWR refractivities, the average STD was 9.3 mm km^{-1} (Ha *et al*., 2010).

A study was conducted on the comparison of GPS PW estimates over Tropical Tahiti Island between two GPS stations (THT I and FAA1) which had a mean slope of 8% and a diameter of 30 km. The altitude difference between the two stations is 86.14 m, and their horizontal distance difference is 2.56 km. The results show that the differences of PW between two nearby GPS stations is nearly a constant with value 1.73 mm (Zhang *et al*., 2019).

A research was conducted on Determination of Atmospheric Water Vapour using GNSS Signals for Numeric Weather Prediction in Tanzania whereby the data from GPS CORS station (DODM) in Dodoma were used. By using two GNSS processing software, gLAB and GAMIT/GLOBK to process data and the results of PW from GNSS were analyzed against each other and against data from Global Reanalysis model of ERA-Interim. The results showed a positive correlation of r = 0.9588 (Mlawa, 2020).

In most developing countries, these Ground Based GNSS stations for meteorological applications have not been employed though there are stations which are currently in use for different geodetic applications in such areas. In Tanzania, a network of Continuously Operating reference frame (CORS) stations has been introduced for different GNSS applications with a total

of 22 ground stations (UNAVCO, 2018) but there has been no engulfing of meteorological advantages from such stations.

1.3 statement of the research problem

Weather forecasting is dependent on accurate observations of the atmosphere surrounding the whole planet, but there is a significant lack of ground-based meteorological observation stations. For example, in Tanzania there are only four radiosondes installed in different regions including the one at Julius Nyerere International Airport (JNIA) in 2004 in which most of them have not been active for recent years and are very expensive. Weather forecasting is sometimes difficult to resolve by global models partly because it occurs at small spatial and temporal scales. However, most rainfall events were not well forecasted by current Global and Regional models whereby this implies that more suitable ways to improve accuracy of the forecast produced and issued to users and the public is required. Currently the available settings of the Global Weather Prediction Model (NWP) do not provide accurate forecasts to meet customer satisfaction for all seasons but the use of GNSS meteorology can fill that gap since the emerging GPS network of continuously operating receivers offer the possibility of observing the horizontal distribution of IWV or, equivalently, precipitable water. These measurements could be utilized in operational weather forecasting and in fundamental research. Therefore, this research shows the retrieval of IWV from CORS stations and analyzing them from global reanalyzed data for numerical weather prediction in Tanzania.

1.4 Objectives of the Research

1.4.1 Main Objectives

To show comparison of water vapor computed from GNSS and Global Weather Models for numerical weather prediction in Tanzania.

1.4.2 Specific objectives

i. Computation of the Precipitate Water (PW) or Integrated Water Vapor (IWV) and generating Time Series to depict pattern.
ii. Comparing PW computed by GNSS from GAMIT/GLOBK software and IWV from Global reanalysis data.

1.5 Study Area

This study used data for a period of one year (1st January 2015-1st January 2016) from the specified GNSS CORS stations which were obtained from UNAVCO, an archive that stores datasets for Tanzania. The stations include ARSH located at latitude -3.387ºS and longitude 36.698ºE, DODM located at latitude -6.187ºS and longitude 35.748ºE and MTVE located at latitude -10.26ºS and longitude 40.166ºE in Tanzania, as well as global atmospheric reanalysis data which is Era-interim. Consider figure 1.1 below showing the study area used in this research.

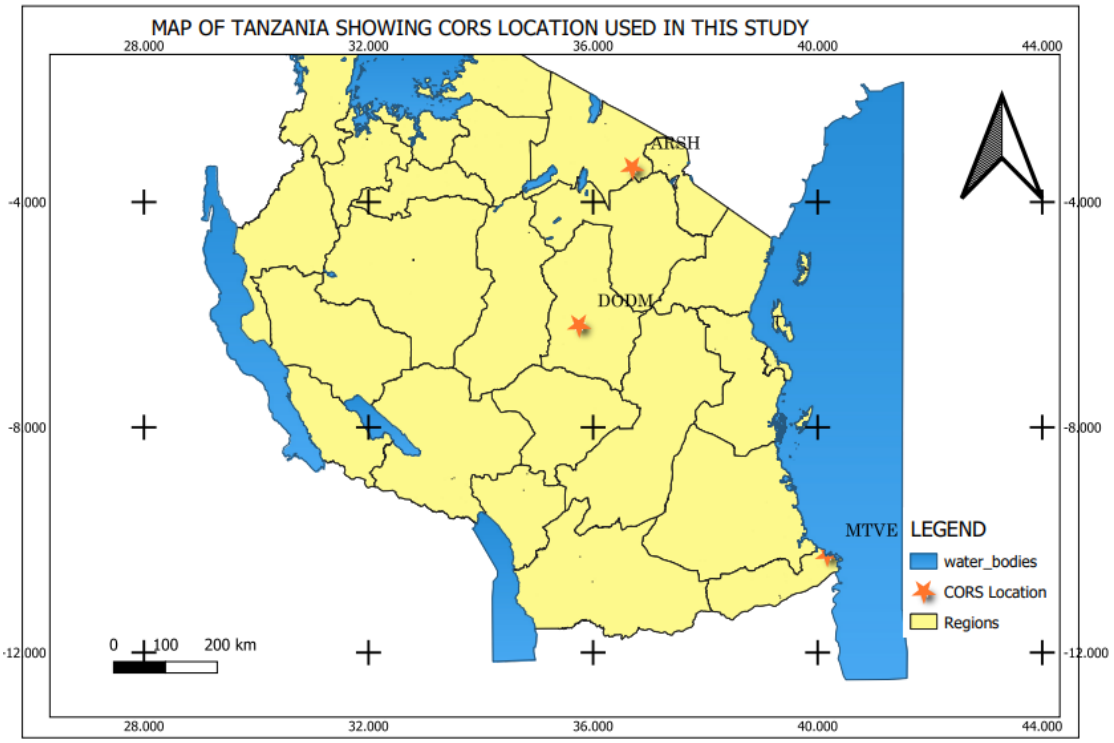

Figure 1. 1 Map of Study area

1.6 Significance and beneficiaries of the research

The research forms a base for GNSS meteorology in Tanzania for weather forecasting by TMA and enhancing improvement of data source and better forecasting. Also, the research stimulates Geomatics students and researchers in doing more research related to atmospheric sciences by using their knowledge on GNSS techniques and so increasing applicability of diversity of the course. Moreover, the Global Upper Air Network (GUAN) may use results from this

research as a key for deciding whether to include IWV data obtained from CORS station in Tanzania to their data accounts.

Meteorologists and scholars may include findings from this research as their source of knowledge and understanding.

1.7 Limitation of the Research

i. The research has limited geographical location since it involves the use of only three CORS stations located at the central, northern and southern part of Tanzania.

ii. This research is not supposed to provide a 3D profile of the amount of water vapour but instead to propose a way for determining water vapour from the atmospheric water vapour parameters which are obtained by GNSS meteorology.

1.8 Organization of the research

This research consists of five chapters. Chapter One covers main concepts regarding atmospheric water vapor with its significance in weather prediction. It gives a brief summary on similar research regarding GNSS meteorology and stating the research problem together with the objectives of research. Chapter Two discusses some important concepts regarding meteorology, water vapour, GNSS, tropospheric delay and statistical analysis techniques from different literatures which are related to this research. Chapter Three gives a detailed methodology used to process and analyze results obtained from this research. Chapter Four, presents the results and discussion of obtained results and finally Chapter Five provides the conclusion and recommendations regarding findings of this research.

CHAPTER TWO

LITERATURE REVIEW

This chapter contains the reviews of the main concepts about this research which are explained in detail for more understanding.

2.1 Meteorology

Meteorology is the part of atmospheric science which includes atmospheric physics and atmospheric chemistry with a major focus on weather forecasting (Weber, 2004). This study includes some concepts from such fields as explained in the following subsection.

2.1.1 Atmosphere

Atmosphere is one of Earth layers consisting of gasses surrounding the Earth which are retained over the globe, by the action of earth's gravity. It contains about 5000 million tons of gasses. Among these, the occurrence of Nitrogen amounts to 78%, oxygen to 21%, carbon-di-oxide to 0.33% and argon to 0.93. The other gasses present in the atmosphere include helium, methane, ozone, neon, xenon and many other trace gasses (Balasubramanian, 2011). These gas constituents can be grouped into three main categories: dry air, water substance, and aerosols (Potter & Colman, 2003).

The Earth's atmosphere consists of five (5) different layers according to their thermal state. Each layer is distinct and can be identified mainly by how temperatures change with increasing height and chemical composition (Leinweber, 2010). The layers are bounded by four (4)" pauses" where appreciable changes in thermal characteristics, chemical compositions, movements, and densities occur. The lowest layer called the troposphere is characterized by a decreasing temperature with respect to height up to the tropopause (≈16km). On top of the troposphere is the stratosphere that is characterized by an increase in temperature up to 50 km due to very strong ozone absorption. Next is the Mesosphere with a ceiling of between 90– 100 km in altitude, temperature decreases with height in this medium. Thermosphere comes next rising from 90 km to 1000 km. Temperatures in this layer can reach up to 2000^{o} K or higher (Bevis *et al*., 1992). It is relatively transparent to incoming ultra-violet solar radiation and opaque to outgoing infra-red radiation emitted by the Earth's surface (Wallace & Hobbs, 2006). This property of scattering radiation or signals propagating through its medium (especially the troposphere) makes a way for this study. Almost all-weather phenomenon occurs in the lowest atmospheric layer, the

troposphere which is relatively unstable and carries approximately 90% of the weight of the atmosphere and with most atmospheric water vapour and aerosol (Pottiaux, 2010). The troposphere is characterized by a constant decrease of the temperature with an atmospheric lapse rate of 6.50 C/km and has an average of 16 km over the equator, 11km in middle latitudes and 8 km over the Polar Regions (Wallace & Hobbs, 2006).

2.1.2 Weather and Climate

Weather refers to the specific condition of the atmosphere at a particular place and time measured in terms of variables including wind speed and direction, air temperature, humidity, atmospheric pressure, cloudiness, and precipitation. Weather can change from hour to hour, day to day, and season to season while Climate is a statistical characterization of the weather, averaged over many years; it is usually represented in terms of means, variability, and extremes of the various weather elements (Spittlehouse *et al*., 2008). Though there may be variability in climate or change, but the climatic pattern of a place is expected to be almost the same for a long time (Weber, 2004).

2.1.3 Weather forecasting

Weather forecasting is the application of Science and Technology to predict the state of the atmosphere for a future time and a given location. Human beings have attempted to predict the weather informally for millennia, and formally since at least the nineteenth century. Weather forecasts are made by collecting qualitative data about the current state of the atmosphere and using scientific understanding of atmospheric processes to project how the atmosphere will evolve within the next few hours (Ise, 2013). A model, in this context, is a computer program that produces meteorological information for future times at given positions and altitudes.

Regional models also are known as limited area models. Human input is still required to pick the best possible forecast model to base the forecast upon, which involves pattern recognition skills, knowledge of model performance and knowledge of model biases. The chaotic nature of the atmosphere, errors involved in measuring the initial conditions, an incomplete understanding of atmospheric processes mean that forecasts become less accurate as the difference in current time and the time for which the forecast is being made increases (Eresmaa *et al*., 2019).

Methods used in Tanzania for Weather Forecasting

i) Persistence forecasting

Persistence forecasting is the easiest method of forecasting which assumes a continuation of the present. It relies upon today's conditions to forecast the weather when it is in a steady state, such as during the summer season in the tropics. This method of forecasting strongly depends upon the presence of a stagnant weather pattern. It can be useful in both short-range forecasts and long-range forecasts (Ise, 2013).

ii) Climatology forecasting

Whereas persistence forecasting is most accurate over short periods (before factors for change have had time to operate), the best estimate of the weather a long time ahead is the average value of past measurements there at that time of day and year. Climatology forecast relies on the observation that weather for a particular day at a location does not change much from one year to the next. As a result, a long-term average of weather on a certain day or month should be a good guess as the weather for that day or month.

iii) Use of Forecasting Models

In the past, the human forecasters were responsible for generating the entire weather forecast based upon available observation. Today, human input is generally confined to choosing a model based on various parameters, such as model biases and performance. Using a consensus of forecast models, as well as ensemble members of the various models, can help reduce forecast error.

Global Weather Prediction Models

Some of the better-known global numerical models are:

i) Global Forecast System (GFS) – Developed by the National Organization for the Atmosphere in America. Output is freely available.
ii) NOGAPS – Developed by the US Navy to compare with the GFS
iii) European Centre for Medium Range Weather Forecasts (ECMWF) – a model run by the Europeans with limited availability
iv) GME – developed by the German Weather Service
v) Intermediate General Circulation model (IGCM) – developed by members of the Department of Meteorology at the University of Reading (Ise, 2013).

In order to issue forecasts, Tanzania uses Numerical Weather Prediction (NWP) products provided by the Global centers obtained through the GFA (Global Forecasting System, USA), ECMWF (European Centre for Medium Range Weather Forecasts).

iv) Nowcasting

The forecasting of the weather within the next six hours is often referred to as nowcasting. In this time range, it is possible to forecast smaller features such as individual showers and thunderstorms with reasonable accuracy, as well as other features too small to be resolved by a computer model. A human given the latest radar, satellite and observational data will be able to make a better analysis of the small-scale features present and so will be able to make a more accurate forecast for the following few hours (Ise, 2013).

2.1.4 Reanalysis Data

Reanalysis is the scientific method for developing comprehensive records of weather and climatic trends over time (CIRES, 2020). In it are observations and numerical models that simulate one or more aspects of the Earth system. Reanalysis data are created by ingesting all available observations at constant time intervals over the period being analyzed using unchanging data assimilation schemes and models (Dee *et al*., 2020). Though there is wealth of data from weather stations, radiosondes, airplanes, and instruments onboard satellites, global coverage is not complete and quality of data may vary from time to time. Purely mathematical interpolation can do this, but does not provide any extra information, as it is un-physical. In reanalysis, physical models are used to provide the extra information resulting in a physically consistent description (Gleisner & Thelji, 2016).

As part of the data-assimilation a physics-based quality control is performed. Reanalysis models use similar model software but assimilate historical data – weather station data going back more than a century is now being assimilated. As more data describing the past is revealed in digitization and archival work, new reanalysis can be calculated. At the same time the descriptions of physical processes in the models are improved by researchers and new re-analyses of the updated body of data become available (Gleisner & Thelji, 2016).

Reanalysis data have a time span of several decades, global coverage and can be obtained in either of these WMO approved formats - GRIB, netCDF and WMO BUFR. It has a 6-hour time resolution and covers 60 vertical levels up to an altitude of 64 km (0.1 hPa) (Uppala *et al*., 2005)

. The follow-on reanalysis ERA-Interim starts in 1979, is being continued in real time, and has a similar vertical resolution and coverage as ERA-40 (Dee *et al*., 2020). In addition, a set of completely new reanalyses are currently in preparation through the ERA-CLIM1 project led by ECMWF. The final global reanalysis, covering the whole 20th century, 1900-2010, is not expected to be finalized before 2017. However, the results of a few specialized reanalysis, e.g., a high-resolution land-surface reanalysis and a 20th century atmospheric reanalysis based only on surface observations, are already available. The ERA-CLIM reanalysis constitutes significant advancements, both in terms of resolution, time coverage (the whole 20th century, 1900–2010), and in the systematic handling and error characterization of the observational data (CIRES, 2020).

The US NCEP/NCAR reanalysis come in two different versions: NCEP/NCAR I, which covers the time span from 1948 to the present, and NCEP/NCAR II, which only covers the major satellite era after 1979 (Potter & Colman, 2003). Data from this reanalysis are available on 17 pressure levels up to 10hPa. The latter reanalysis incorporates more observational data and addresses some deficiencies in the older data assimilation system. For the satellite era, 1979 and onward, there is also the NCEP CFSR reanalysis, which is unusual in the sense that the reanalysis is done with a fully coupled atmosphere-ocean-land surface-sea ice model to provide an optimal estimate of the state of these coupled domains (Dee *et al*., 2020).

The Japanese Meteorological Agency has also produced a set of global atmospheric reanalysis: the 55-year reanalysis JRA-55 with 60 vertical levels, and the 25-year reanalysis JRA-25 with 40 vertical levels (Dee *et al*., 2020).The former started in 1958 and the latter in 1979. Both are currently undergoing an update to the present. While these three reanalysis projects are the most widely used, there are also others available, some of them more specialized. MERRA3 is a NASA reanalysis covering the satellite era. It has partly a focus on the hydrological cycle and water vapour, and has been used extensively for water-vapour budget studies. NOAA has produced a 20th century reanalysis4, covering the time 1871–2012. It has a 6-hourly time resolution, covers both the troposphere and part of the stratosphere, and data is provided on a 2-degree grid. A more specialized data set is the Arctic System Reanalysis (ASR), covering the Arctic region at a high spatial resolution (Dee *et al*., 2020). Table 2.1 shows the reanalysis models consisting with their names, developers, time steps and model resolutions.

Table 2.1 Overview of Reanalysis models

Name	Developers	Time steps	Model Resolution
Climate Forecast System Reanalysis (CFSR)	NCEP	Sub-daily	0.5º x 0.5º & 2.5º x 2.5º
		Monthly	0.266 hPA top
ERA-Interim	ECMWF	Sub-daily	0.125º x 0.125º x 60 levels
		Monthly	0.1 hPA top
JRA-55	Japanese Meteorological Agency	Sub-daily	0.562º x 0.562º x 60 levels
		Monthly	0.1 hPA top
NASA MERRA	NASA	Sub-daily	0.5º x 0.667ºx 72 levels
		Monthly	0.1 hPA top
NCEP Reanalysis (R2)	NCEP, DOE	Sub-daily	2.5º x 2.5º x 28 levels
		Monthly	3 hPA top
NCEP Reanalysis (R1)	NCEP, NCAR	Sub-daily	1.875º x 1.935º x 28 levels
		Monthly	3 hPA top

2.2 Tanzania Meteorological Agency (TMA)

Tanzania Meteorological Agency (TMA) is a Government Agency established by the Government Executive Agency Act no.30 of 1997 and it was then officially launched on 3rd December 1999 the Agency is responsible for the provision of Meteorological services; weather forecasts, climate services and warnings and advisories information for the country. Tanzania Meteorological Agency is currently operating under the Ministry of Works, Transport and Communications of the United Republic of Tanzania (TMA, 2021).

Observations of Meteorological data in Tanzania first began along the coast. The first weather observations were made at the Zanzibar stone town in October 1886 and later extended to the mainland with the rainfall observing stations being Bagamoyo, Tanga, Amani and Bukoba. By 1929 meteorological services had become fully operational in Tanzania under the British Meteorological Services. Today observed meteorological parameters are Rainfall, Maximum, Minimum, Dry bulb, Dew Point, Wet bulb temperatures, Cistern Level Pressure, Relative Humidity, Vapor Pressure, Cloud Cover, Evaporation, Radiation, Sunshine hours, Wind run, Wind

Speed, Wind Direction, Fog, Thunder, Hail, Mean Sea Level, Visibility and Evaporation (TMA, 2021).

2.2.1 Meteorological Observation Techniques

Meteorological observations are made for a variety of reasons. They are used for the real-time preparation of weather analyses, forecasts and severe weather warnings, for the study of climate, for local weather dependent operations (for example, local aerodrome flying operations, construction work on land and at sea), for hydrology and agricultural meteorology, and for research in meteorology and climatology (WMO, 2018).

The requirements for observational data may be met using in situ measurements or remote-sensing (including space-borne) systems, according to the ability of the various sensing systems to measure the environmental elements needed. The space-based subsystem comprises a number of spacecraft with on-board sounding missions and the associated ground segment for command, control and data reception (WMO, 2018). The data from remote sensing are further categorized into remote sensing from satellite platforms and remote sensing from ground station and most widely used in situ observations are wind speed and direction, pressure, temperature, humidity (Acheampong A. A., 2015). GNSS observation from ground stations shown in Table 2.2 is one of remote sensing from ground station techniques of weather measurement.

Weather observations are normally taken on the major synoptic hours (0000, 0600, 1200, and 1800 UTC), but three-hourly intermediate observations are necessary at some in- stances (NWS-Editors, 2004). Several meteorological quantities that can be derived by combinations of independent measurements from separate instruments at areas of interest or from regions which have highly correlated physical ground condition and so data retrieved from satellites must be compared with actual reports of surface variables to confirm developing patterns (Potter & Colman, 2003).

Table 2.2 Weather Observation Techniques

Observing technique	Weather parameter
Surface Measurement	Temperature, pressure, wind speed, precipitation wind, wind direction, humidity, dew point
Radiosonde	Upper air data
Ground water Radar	Precipitation and water droplet motions
Water vapour Radiometer	Vertical humidity profile
Light Detection and Ranging (LIDAR)	atmospheric gasses, clouds, and aerosols
Aircraft Meteorological Data Relay (AMDAR)	Air temperature, wind speed and direction, Pressure, Turbulence, Water Vapour
GNSS	Integrated water vapour or precipitable water vapour
Satellites	heat balance, weather fronts, storm locations, radiance, Humidity, cloud cover temperature
Ships and Buoys	Radiance, Humidity, cloud cover, temperature

2.2.2 Numerical Weather Prediction

Numerical Weather Prediction data are the most familiar form of weather model data. NWP computer models process current weather observations to forecast future weather. Output is based on current weather observations, which are assimilated into the model's framework and used to produce predictions for temperature, precipitation and hundreds of other meteorological elements from the oceans to the top of the atmosphere (Haan, 2011). Modern Numerical Weather Prediction (NWP) models make use of the GNSS-derived Zenith Total Delay (ZTD) or Integrated Water Vapour (IWV) estimates to enhance the quality of their forecasts. Using present GNSS products and tools, ZTD can be estimated in realtime (RT), near real-time (NRT) and post-processing (PP) modes (Ahmed *et al*., 2015).

2.3 Water Vapour

Water is the only substance in the Earth's environment that exists naturally in significant quantities in all three states: solid (ice), liquid (water) and gas (water vapour) (Shakhashiri, 2010). Water in its gaseous phase (water vapour) moves on a global scale transporting enormous amounts of latent heat energy to maintain the Earth's energy balance. Water vapour gets to the atmosphere through open-water evaporation (from the ocean, lakes and rivers), land surfaces, sublimation from ice and snow surfaces and evapo-transpiration from vegetation. This cycle takes approximately between 7 to 10 days; the movement includes vertical and horizontal transports, mixing, condensation, precipitation and evaporation (Guerova, 2003). Water vapour is one of the key prognostic variables in numerical weather prediction (NWP) models as well for climate models. Water vapour has a high temporal and spatial variability (Leinweber, 2010) and so accurate measurements in highly temporal and spatial resolutions are essential for the initialization of NWP models for accurate predictions/forecasting. Water vapour density, water vapour mixing ratio, specific humidity and relative humidity are various definitions used to quantify the amount of water vapour in air (De haan, 2008). The total amount of water vapour in a vertical column which is widely used in meteorology is expressed using Total Precipitable Water (TPW) or Integrated Precipitable Water (IPW) or Integrated Water Vapour (IWV) (Acheampong A. A., 2015).

2.3.1 Water vapour measurement techniques

Data for water vapour have been obtained by use of different techniques in which its measurement still has not been enough as compared to its neediness as explained in chapter one of this research. Such techniques include radiosondes (RAOBs), microwave radiometers (MWRs), remote sensing satellites, and the Global Positioning System (GPS) (Ha *et al*., 2010).

The radiosonde is composed of a meteorological sensor and a balloon, and the sensor measures pressure, temperature, and humidity as it soars up with the balloon. Based on radiosonde observation one can get vertical profiles of the atmosphere from the surface through to the upper atmosphere. In real-world situations, however, winds can cause the balloon to drift away from the zenith direction at the launch site. In those cases, the radiosonde measurements cannot provide a 'true' vertical. Currently, a radiosonde is the most widely used water-vapor measuring device. About 900 World Meteorological Organization radiosonde stations, under the World Weather Watch program, launch radiosondes several times a day (Ha *et al*., 2010).

Microwave radiometers (MWRs) detect water vapor and cloud liquid water in the atmosphere by measuring the brightness temperature of the atmosphere at frequencies of 1832 GHz. Some old MWR models, such as the WVR-1100 manufactured by Radiometric, observe only the total amount of water vapor along its line of sight.

Remote sensing satellites can measure water vapor by observing the brightness temperature of the atmosphere using onboard infrared and microwave sensors. Microwave sensors can measure water vapor even under cloud, but they only work in oceanic parts of the Earth (Ha *et al*., 2010).One of the disadvantages of satellite-based measurements is that one cannot use infrared sensors to retrieve data on water vapor content under clouds and even though microwave sensors can measure water vapor even under cloud, but they only work in oceanic parts of the Earth because of their relatively simple surface condition (Zhou *et al*., 2016).

GNSS meteorology, from GPS measurements, one can determine the amount of signal delay due to the atmosphere. Then, the time delay due to water vapor can be separated from the total delay with the use of on-site pressure and temperature measurements (Ha *et al.*, 2010). The GNSS meteorology (before GPS meteorology) was suggested by (Bevis *et al*., 1992) and later in 1997; it was clarified more by (Solheim & Ware, 1999). The concept is based on propagation delays due to a neutral atmosphere as the magnitude of signal delay was treated to be proportional to the amount of water vapour in the atmosphere (Bevis *et al*., 1992). The delayed GPS signals by atmosphere and ionosphere are considered as errors and not needed in geodetic applications but interestingly they become useful atmospheric parameters when well modeled (Schüler, 2001). As this technique is seen to cover a lot of deficiencies of other techniques, this research uses GNSS approach to retrieve water vapour in terms of Precipitable water vapour from GNSS CORS stations in Tanzania.

2.4 GNSS

Global Navigation Satellite System (GNSS) is the basis for many novel geodetic positioning applications. The two currently available navigation satellite systems are the Global Positioning System (GPS) and the Globalnaja Navigatsionnaja Sputnikovaja Sistema (GLONASS) maintained by the US and the Russia, respectively. The Galileo navigation satellite system, which is under development by the European Space Agency (ESA), is expected to be completed within the time

frame of a few years. Ground-based GNSS meteorology is an example of a scientific application taking advantage of the GNSS. Since dense GNSS receiver networks can be built at a low cost and they can provide observations with high temporal frequency, the meteorological potential of such a new observing system is high (Eresmaa R. , 2022).

2.4.1 Meteorological GNSS Observation

According to the definition used in the geodetic literature, the tropospheric delay Δ^T is an integral of refractivity N along the path s taken by the microwave signal through the atmosphere (Hofmann-Wellenhof, 2001).

$$\Delta^T = 10^{-6} \int N ds \quad \text{..... Eq (2.1)}$$

Refractivity N of the neutral air is governed by pressure p, temperature T and specific humidity q according to

$$\frac{k1P}{T} + \frac{(K2-K1)qp}{(0.622+0.378q)T} + \frac{K3qp}{(0.622+0.378q)T^2} \quad \text{..... Eq (2.2)}$$

where the refraction coefficients are k_1=77.60 *K/hPa*, k_2=70.4 *K/hPa* and k_3=3.739 x 10^5 K^2/hPa (Bevis M. a., 1994)

2.5 Time Series Analysis

Time series analysis refers to the analysis used to analyze a set of statistical data collected at an interval of time. This analysis comprises methods for analyzing the time series data which can either be a continuous trace or a set of discrete observations. Time series analysis is very important in many applications, this can be applied in environmental studies. for example, daily rainfall and temperature, economics, finance and medicine. The aims of time series analysis are to describe and summarize time series data and make forecasts (Borkowf, 2002). The characteristics and variations of the time series data are more expressed in terms of graphs.

2.6 Correlation Analysis

Correlation is used to show the relationship between two or more quantitative variables (Gogtay & Thatte , 2017). Correlation shows the degree and direction to which the two or more variables are related to each other by computing the correlation coefficient (r) which tends to show on how much one variable changes when the other does. The correlation coefficient is range between +1 and -1, if the correlation coefficient appears to be +1 indicate that the two variables

are related to each other in a positive way and if the correlation coefficient (r) obtained to be -1 this indicate that the two variables are related to each other in a negative way and if the correlation coefficient is obtained to be 0 this means that there is no relationship between the two variables. A positive indicates the extent to which the two variables increase or decrease in parallel and the negative correlation indicates the extent to which one variable increases as the other one decreases (Shi, 2009).

There are three types of correlation coefficient;

i. Pearson correlation coefficient.

This is the correlation which is more used in statistics to measure the degree of relationship between the linear related variables. The Pearson correlation coefficient (*r*) can be computed through the Eq (2.3) below;

$$r = \frac{\sum_{i=1}^{n}(xi-\bar{x})(yi-\bar{y})}{\sqrt{\sum_{i=1}^{n}(xi-\bar{x})^2 \sum_{i=1}^{n}(yi-\bar{y})^2}} \quad \text{..... Eq (2.3)}$$

Whereby ***r*** is the Pearson correlation coefficient, *is* the mean of variable *x* and is the mean of variable *y.*

ii. Kendall's Tau rank correlation coefficient.

This is the correlation which is a non-parametric test that can be used to the strength of dependence between the two variables. And this coefficient is obtained from the equation 2.4

$$\tau = \frac{nc - nd}{0.5\, n(n-1)} \quad \text{..... Eq (2.4)}$$

Whereby τ is the Kendall's rank correlation coefficient, nc is number of concordant (ordered in the same way) and nd is number of discordant (ordered in differently).

iii. Spearman rank correlation coefficient.

This is also a non-parametric test that can be used to measure the degree of association between the two variables. The test in this correlation does not have any assumption about the distribution of the data and is the appropriate correlation analysis when the two variables are measured on a scale that is at least ordinal (Shi, 2009).

2.7 Related Studies

(Jiang *et al*., (2016), investigated for Retrieving Precipitable Water Vapor Data Using GPS Zenith Delays and Global Reanalysis Data in China, in research they use The NCEP FNL dataset provided by the NCEP (National Centers for Environmental Prediction) and over 600 observed stations from different sources were selected to assess the quality of the results. A one-year experiment was performed in this study. The types of stations selected include meteorological sites, GPS stations, radio sounding stations, and a sun photometer station. The results of this experiment were at more than 96% of selected stations, PWV differences caused by the differences between the interpolation results and real measurements were less than 1.0 mm and study indicates that GPS PWV products that use interpolated surface meteorological elements were very close to those based on real meteorological observations, with differences within ±0.4 mm and a RMSE mainly below 0.6 mm.

A research was conducted on Determination of Atmospheric Water Vapour using GNSS Signals for Numeric Weather Prediction in Tanzania whereby the data from GPS CORS station (DODM) in Dodoma were used. By using two GNSS processing software, gLAB and GAMIT/GLOBK to process data and the results of PW from GNSS were analyzed against each other and against data from Global Reanalysis model of ERA-Interim. The results showed a positive correlation of r = 0.9588 (Mlawa, 2020).

The National Institute of Meteorological Research of Korea conducted PROBEX2009 (Predictability and Observation Experiment in Korea) in Ulleungdo from August 20 through September 30 and water vapour profiles for 14 days 2009 including periods of severe weather condition were estimated from MWR, GPS and RAOB. In particular, the standard deviation of wet refractivity profiles between GPS with MWR was smaller than the STD between RAOB and MWR refractivities, the average STD was 9.3 mm km^{-1} (Ha *et al*., 2010).

A research was conducted on comparison of GPS PW estimates over Tropical Tahiti Island between two GPS stations (THT I and FAA1) which had a mean slope of 8% and a diameter of 30 km. The altitude difference between the two stations is 86.14 m, and their horizontal distance difference is 2.56 km. The results show that the differences of PW between two nearby GPS stations is nearly a constant with value 1.73 mm (Zhang *et al*., 2019).

CHAPTER THREE

METHODOLOGY

This chapter contains the methods and steps followed to obtain the results. It includes the identification of the data, the sources which are used to acquire the data, the format and quality check of the data, data processing, data analysis and interpretation of the results obtained. The methodology is focused in determining the atmospheric water vapour from the GPS signals by using a GPS processing software and later a performance comparison was performed against a global reanalysis data ERA-interim.

3.1 Data Identification

The data were identified based on where they were used so as to later fit in required objectives. The data included GNSS datasets and meteorological data for the CORS stations. Table 3.1 gives a detailed summary on identified data with their sources, data format and where they were used.

Table 3.1 Data Identification for the Research

DATA	FORMAT	SOURCE	USE
GNSS observation and navigation files for CORS and IGS station for 1 year (January 2015-January 2016)	Compressed RINEX (HATANAKA) xxxxsddd.yy.d. z	UNAVCO https://www.unavco.org/data/gps-gnss/data-access	PPP processing
GNSS Meteorological files for CORS station for 1 year (January 2015-January 2016)	RINEX xxxxsddd.yy.m.z	UNAVCO https://www.unavco.org/da ta/gps-gnss/data-access	ZWD, PW and IWV computation
GNSS precise ephemeris and precise clock	cccwwwd.sp3.z cccwwwd.clk. z	CDDIS ftp://cddis.gsfc.nasa.gov/ pub/gps/products/	For PPP processing
IWV from global reanalysis data.	NetCDF files	ttps://cds.climate.copernicus.eu/cdsapp#!/dataset/reanalysis-era-interim-pressure-levels?tab=form	Validation and statistical analysis of IWV from CORS

3.2 Data Source and Acquisition

Data used in this research were acquired from different international sources and different formats as explained below;

3.2.1 RINEX observation, meteorological, navigation files for experiment sites and RINEX observation files for IGS sites.

All downloaded data from UNAVCO were in compressed format (. z) and furthermore, RINEX observation files were first crinexed (hatanaked (. d)). The data format RINEX observation, meteorological and navigation files were xxxddds.yyd.z, xxxddds.yym.z and xxxddds.yyn.z respectively in which xxxx is station marker name, ddd is day of year,s is session, yy are last two digits of year, d,n,m are file typs. The IGS sites downloaded includes ABPO, ADIS, DEAR, HARB, MAL2, MSA1, SUTH, NKLG, SEY, REUN, MBAR.

Below is Figure 3.1 showing the Earthscope Consortium data download center where Rinex observation and meteorological files were downloaded with an example of ABPO IGS site.

ABPO - Data Download Options <<< Back to ABPO Search Result Page

NOTICE - By downloading data from UNAVCO, you are agreeing to abide by the acknowledgments section of the UNAVCO Data Policy.

Data Type Download Option	Estimated File Count	Estimated File Size	Start Time	End Time	Choose Option
RINEX Data					
All RINEX Data Individual File Links (hatanaka, obs, nav, qc)	4649	~4649MB	2007-11-16	2023-04-23	Bundle Data
Time-Windowed RINEX Data	361	~361MB	2015-01-01	2015-12-31	Bundle Data
Latest RINEX Data File	1	~1MB		2023 Apr 23 23:59:30	Download

Figure 3.1 EarthScope Consortium Data Download Center

3.2.2 Integrated water vapor (IWV) from Global reanalysis data

The vertical integral of water vapor was downloaded from ECMWF of class ERA-Interim in which daily data with resolution of 0.125º*0.125º at mainly synoptic hours 00:00:00, 06:00:00, 12:00:00, 18:00:00 was retrieved in NetCDF file format. The data from ERA-Interim were downloaded from 1st/January/2015 to 31st/January/2016. These data can be downloaded from the link https://cds.climate.copernicus.eu/cdsapp#!/dataset/reanalysis-era-interim-pressurelevels

3.2.3 Precise ephemeris and precise clock files

The final satellite position files (precise ephemeris) in sp3 format and precise clock files in clk format were downloaded from data archives covering the interval specified above by corresponding the GPS week and day and so these data were from GPS. The precise ephemeris files were downloaded using get_orb command with help of GAMIT/GLOBK software from data archives of cddis and corresponding clock files were downloaded through file transfer protocol (ftp) from cddis with the link ftp://cddis.gsfc.nasa.gov/pub/gps/products/. The downloaded precise ephemeris and clock files were in cccwwwd.sp3.z and cccwwwd.clk.z respectively in which ccc-three letter ID for the centre which generated the file wwww-four digits GPS week d-single digit day of week 0=Sunday, 1=Monday…6 sp3/clk-file type.

3.4 Data Format

The acquired data were prepared so as to meet requirements of specific tasks in need to accomplish this research objective. Data were manipulated in terms of changing their file type (extension), arranging them, finding mean and extracting them from different formats so as they can be read by software under research.

3.4.1 RINEX observation files for experiment and IGS sites.

The rinex data was in HATANAKA format. The data format of RINEX observation, meteorological and navigation files were xxxddds.yyd. z, xxxddds.yym.z and xxxddds.yyn.z respectively in which xxxx is station marker name, ddd is day of year, s is session, yy are last two digits of year, d,n,m are file types. Observation files of all stations were acquired in compressed and crinexed format (xxxddds.yyd. z), and so data were first uncompressed using windows winRAR app to remove. z and then the hatanaked file (xxxddds.yyd) were uncrinexed to get xxxddds.yyo observation files by using CRX2RNX_4.08 app in windows command line as shown in Figure 3.2.

```
C:\Users\SIGN IN\Downloads\dissertation\2015\arsh\arsh new>crz2rnx *.15d
Option settings
-------------------------------
output to current path:   NO
delete input files:       NO
keep output when failed:  NO
skip the file with error: NO
-------------------------------
"(type arsh0010.15d  | CRX2RNX - & call echo %^ERRORLEVEL% > tmp_errlvl_29955.log ) > arsh0010.15o"
"(type arsh0020.15d  | CRX2RNX - & call echo %^ERRORLEVEL% > tmp_errlvl_29955.log ) > arsh0020.15o"
"(type arsh0030.15d  | CRX2RNX - & call echo %^ERRORLEVEL% > tmp_errlvl_29955.log ) > arsh0030.15o"
```

Figure 3.2 Uncrinexing Hatanaka files using crx2rnx

3.4.2 RINEX meteorological file

The RINEX meteorological files were first uncompressed using windows WinRAR app to get its uncompressed file (xxxxddds.yym) so as to be read by GAMIT/GLOBK software.

3.4.3 IWV from Global reanalysis data (ERA-Interim)

The data of vertical integral of water vapor from ERA-interim were acquired in netCDF files (.nc) and so they were first converted into excel .xlsx file format.

input xxxxxx.nc to NetCDF4Excel_2015.xlsm→ xxxxxx.xlsx

After being converted into excel files, the data were then manipulated to get weighted daily mean of the interpolated value from four (4) corners of 0.125º*0.125º grids of downloaded data and four sets of data at each synoptic hour to get the most probable value at the experiment site. The data were unweighted considering the data at each synoptic hour (00:00:00, 06:00:00, 12:00:00 and 18:00:00) but weighted considering the distance from the experiment site to corner points of gridded data which will be shown in Appendix I.

3.5 Data Processing

After preparing all necessary data for processing and arranging them in respective folders for each year (rinex, brdc, gsoln, igs and meteofiles), the data were subjected to GAMIT/GLOBK processing. GAMIT/GLOBK is a comprehensive GPS analysis package developed at MIT, the Harvard Smithsonian Centre for Astrophysics (CfA), Scripts Institution of Oceanography (SIO), and Australian National University for estimating station coordinates and velocities, stochastic or functional representations of post-seismic deformation, atmospheric delays, satellite orbits, and Earth orientation parameters (Herring et al., 2015).

3.5.1 Creating working directory

Since the data processed include one year then one top directory was set up for year 2015. In the year directory, five directories were set up where the data for processing were inputed which were rinex, meteofiles, igs, brdc and gsoln as shown in Figure 3.3.

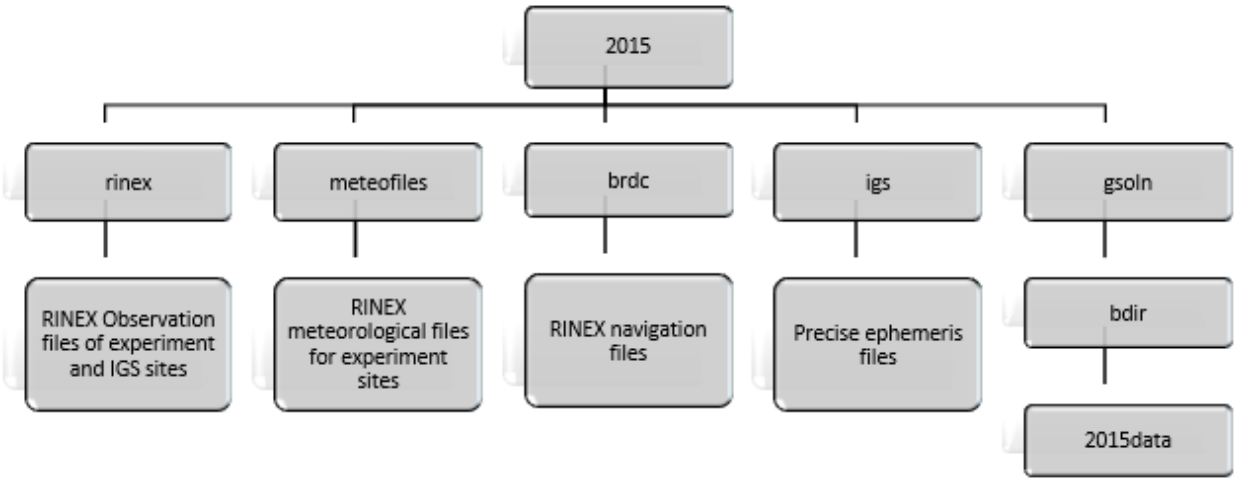

Figure 3.3 Workflow for processing GNSS Data by using GAMIT Software

3.5.2 Creation of tables

The gamit tables directory was set up on the year directory runned by *2015> sh_setup -yr. 2015.* This copies the default tables/ folder from ~/gg/ for gamit to get started. All the setup and metadata information for the year 2015 goes here. The created tables directory contained several files with different station information including *lfile., lfile.old, igs14_comb.apr, station.info* and other files.

3.5.3 Updating site information on statio.info file

Before updating this info, the rinex files for all sites which were going to be processed were checked and made sure are in the rinex directory. The following command was used to create the station.info *tables>sh_upd_stnfo -l sd* and the output was *station.info.new* then it was renamed as station.info. Then the station.info file was updated using experiment and IGS sites from the rinex directory using a command sh_*upd_stnfo –files. /rinex/*.15o* which extracts information from the RINEX header for each site in respective year.

3.5.4 Running sh_gamit to get O-files

After the completion of creating and updating the table directory then the tool sh_gamit which contain several GAMIT processes to create daily constrained and loosely estimates were run at year level directory. Before running the sh_gamit command, the orbital information/ final orbit and satellite navigation were checked to make sure they are placed in igs/directory and brdc/directory.The sh_gamit command was as follows

sh_gamit –expt test –d [yyyy] [ddd] –pres ELEV –orbit IGSF –copt x k p –dopt c ao whereby the name of the experiment site was set as *test*. The command was executed for each day for all sites.

The following are the steps which were carried out when sh_gamit was running

i) Assign parameters of program flow, giving precedence first to the command-line arguments, then to the parameters set in process. Defaults and sites. Defaults, and then to default assignments within sh_gamit itself.
ii) Create the day-directory and/or standard directories which do not yet exist.
iii) Link into the day directory the standard tables sing script links. Day and the RINEX files that contain data at 24 hrs interval.
iv) Run makexp to create the input files for makex (scal. makex. Batch) and fixdrv.
v) Run sh_check_sess to make sure that all of the satellites included in the RINEX obs files are present in the nav file and in the g-file (created previously at MIT from an IGS sp3 file).
vi) Run sh_make to create a j-file of satellite clock estimates from the sp3 file.
vii) Run makex to create x-files (observations) and k-files (receiver clock estimates) using phase and pseudorange data from RINEX obs,nav and j-file.
viii) Run fixdrv to create the batch file for GAMIT processing.
ix) Execute the batch run to generate a tabular orbital ephemeris (arc), model the phase observations (model), edit the data (autcln), and estimate parameters (solve) and save the cleaning summary.
x) Create sky plots of phase residuals and plots of phase vs elevation angle using the DPH files written by autcln. xi. Invoke sh_cleanup to delete or compress files as specified by -dopt and -copt.

By following these steps, the outputs obtained contained a lot of files which were the result of this operation whereby the O-files were the files of interest. The O-files contain the parameters of the piecewise-linear model estimated from the data, which met_util will interpolate to obtain ZTD which is the information for the input of the utility sh_metutil (Herring et al., 2015).

3.5.5 Running the utility sh_metutil

After obtaining the O-files as an output from sh_gamit then the following step was running the sh_metutil to obtain the estimated atmospheric values. The o-files were copied into the meteofiles directory which also contained the RINEX met files xxxxddds.yym. The utility sh_metutuil was then run whereby the inputs were the o-files and RINEX met files and then to obtain the output file which will be in the format of met_[site]. [yyddd]. The Utility sh_metutil was as follows *sh_metutil -f testa [ddd] -m [site] [ddd]*.

The scripts induced were of three different parts which covered the whole year of 365 days which were created for the repetition of each process for all days. The prepared scripts were named as srk1.csh, srk2.csh and srk3 for day 1-9, day 10-99 and day 100-365 respectively.

The output files contained ZTD, ZHD, ZWD and PW together with their uncertainties and so the macro 'pwgamit' was recorded to get a weighted mean of daily PW values for each day after renaming all outputs from *met_[site]. [yyddd]* to site *met_[site]. [yyddd].csv* to get excel files. The daily PW were used in statistical analysis with IWV from ERA-Interim.

3.6 Analysis on computed PW/IWVs

Different statistical analyses were performed on daily computed values of PW from GAMIT/GLOBK. These values first were subjected to time series analysis in which they plotted against day of year from 1st/January/2015 to 1st/January/2016 and then descriptive statistics with μ as mean, σ as the standard deviation, maximum and minimum values and range were run on the IWV values from all three sources. The analysis started with analyzing the computed values from GPS signals separately then analyzing them against each other. Finally, the tests were performed against the data From Global reanalysis data of ERA-Interim for each computed PW and lastly the mean of PW computed from GPS signals was analyzed against values from ERA-Interim. Furthermore, the correlation analysis using Pearson correlation coefficient was computed between PWs from GAMIT/GLOBK and ERA-Interim with each other.

CHAPTER FOUR

RESULTS AND ANALYSIS

In this chapter, the results from different processes such as time series, correlation analysis and descriptive statistics are discussed based on the needs of this research. The discussion is based on the comparison of the PW which were the expected end results of this research and the PW from the global reanalysis data Era-interim.

4.1 GNSS Precipitable Water Vapour

The time series analysis of PW from GAMIT/GLOBK software also depends on surface meteorological observation stored in the RINEX met file.

4.1.1 Time series analysis of the computed Precipitable Water Vapour

The results of the daily average Precipitable Water Vapour for the years 2015 observed from three (3) tracking stations namely: ARSH, DODM and MTVE is presented in Figure 4.1.

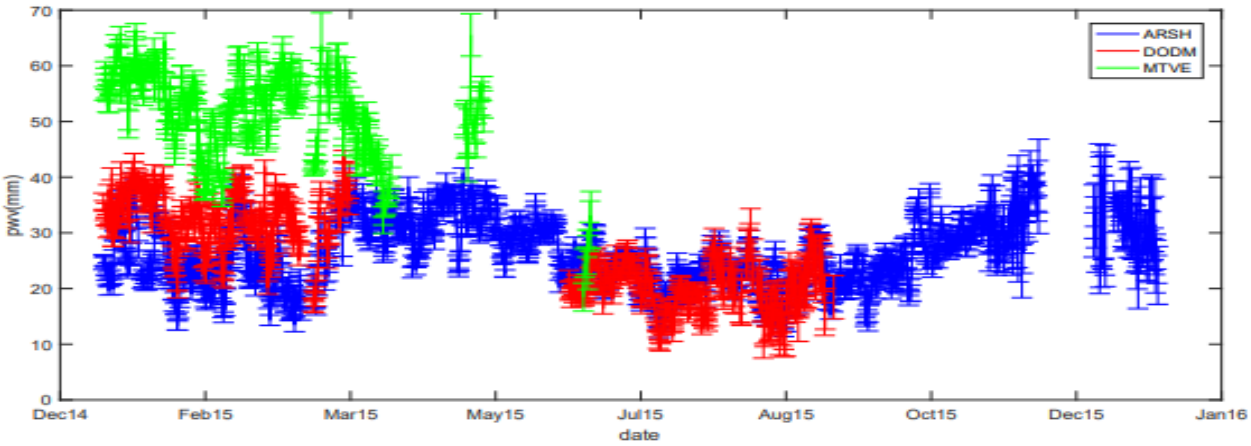

Figure 4.1 Time series showing the computed PW from GNSS Cors station

From Figure 4.1, it shows that there are some irregularities and missing data from the stations whereby these irregularities can be attributed due to missing navigation and meteorological data which is caused by maintenance and hardware changes in GPS and meteorological instruments which resulted in gaps as shown in Figure 4.1. The ARSH time series shows a small missing gap of data from late November to early December 2015. DODM time series shows a large missing gap of data from late March to early June 2015, also from early September to December 2015. MTVE time series shows a significant missing gap of data from early April to early May, late May to late December 2015. Due to the presence of these data gaps,

it's difficult to depict the daily time series for a full year and this results in insufficient assessment of the overall accuracy of the data.

4.1.2 Descriptive analysis of the computed PW

Table 4.1 gives the descriptive analysis of the three Cors stations which are DODM, ARSH and MTVE.

Table 4.1 Descriptive Analysis of the computed PW

	PW_{ARSH} (mm)	PW_{DODM} (mm)	PW_{MTVE} (mm)
μ	26.588	26.450	51.340
σ	5.868	7.917	7.957
max	41.930	43.810	66.400
min	11.930	9.500	18.460
rang	30.000	34.310	47.940

From Table 4.1, the minimum daily average value of PWV for the year 2015 are 11.93mm, 9.5mm and 18.46mm for ARSH, DODM and MTVE respectively. The maximum daily average values of PWV for the year 2015 are 41.93mm, 43.81mm and 66.4mm for ARSH, DODM and MTVE respectively. The station with the minimum daily value of PWV is DODM which falls within the temperate region of the country and the station with the maximum daily value of PWV is MTVE falls within the tropical region of the country where rainfall is high.

4.2 The IWV from global Reanalysis data of ERA-Interim

The downloaded data of IWV from ERA-Interim were analyzed after being spliced into daily data and converted into PW based on time series analysis and their descriptive statistics from 1st/January/2015 to 1st/January/2016.

4.2.1 Time series analysis on PW of Era-interim

The temporal pattern of the precipitable water vapour (PWV) from reanalysis data of Era-interim of each station ARSH, DODM and MTVE respectively was plotted for an interval of one year from 1st January 2015 to 1st January 2016. The trend in Figure 4.2 was continuous throughout the interval with no missing data.

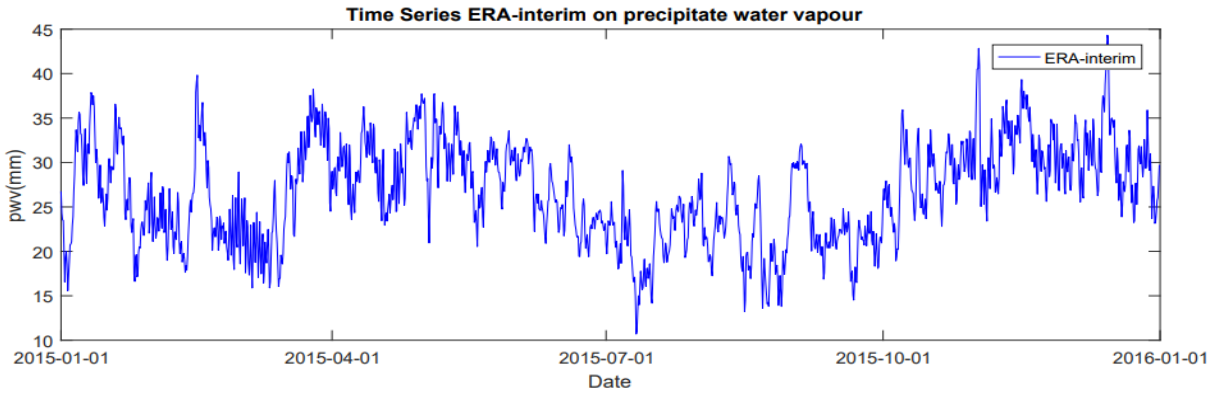

Figure 4.2 PWERA-interim for ARSH Cors station

From Figure 4.2, the overall trend of PW downloaded from ERA-Interim (with some irregularities) shows the high values from March to May and from November to December also comparatively small values from June to the start of October and January to February. This shows the correspondence with Arusha weather pattern whereby it has got two wet and two dry seasons whereby the long rainfall season is from March to May. The short rainfall season is from November and December. The long dry season is from June through October and August is typically the driest month of the year. The short, hot, dry season is in January and February with sporadic rains.

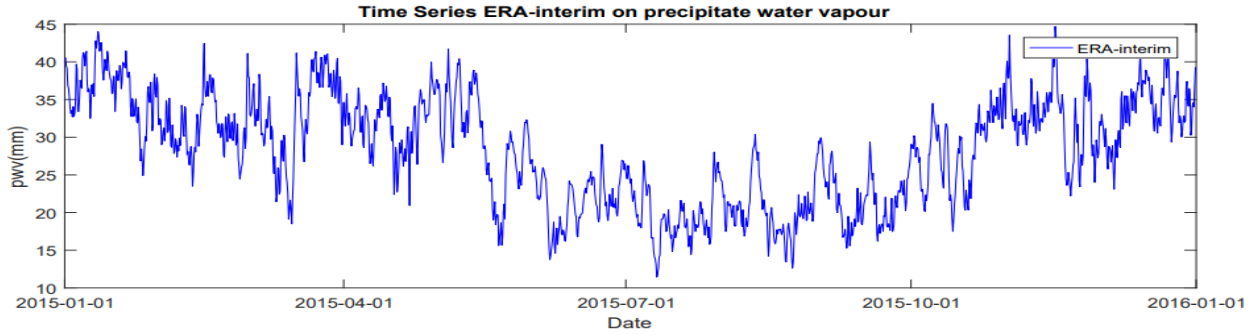

Figure 4. 3 PWERA-interim for DODM Cors station

From Figure 4.3, the overall trend of PW downloaded from ERA-Interim (with some irregularities) shows smaller values between May to the start of November which shows correspondence with the weather pattern of Dodoma in which the dry season is from May to

November. Also, the wet season is from November to May which correspond to the larger values shown in the figure above whereby the high values are between November to April.

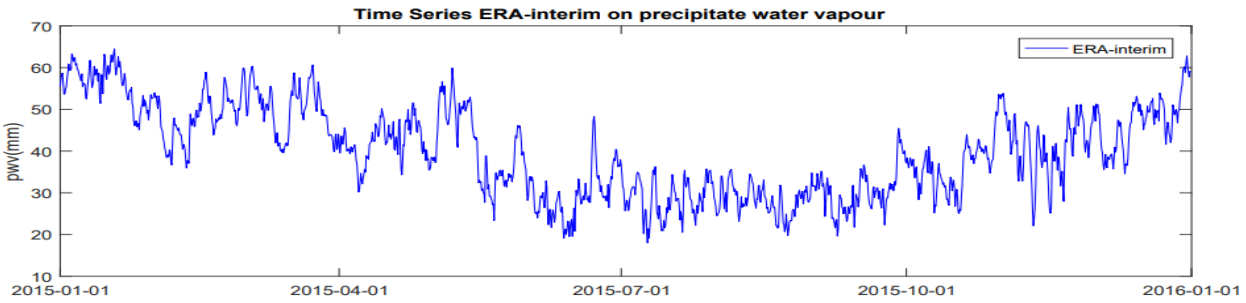

Figure 4. 4 PWERA-Interim for MTVE Cors station

From Figure 4.4, the overall trend of PW downloaded from ERA-Interim (with some irregularities) shows the smallest value in June to the start of October and the highest value from the start of November to the start of May. Mtwara is located in a temperate zone hence makes it difficult to categorize the seasons. According to the trend this corresponds to the weather pattern of the Mtwara region whereby the wet season is from December to the start of May as the months with the high values and the dry seasons is from May to the start of December as the smallest values in the time series.

4.2.2 The descriptive analysis of $PW_{ERA\text{-}Interim}$

Table 4.2 gives the descriptive analysis of the three Cors stations which are DODM, ARSH and MTVE from reanalysis data ERA-Interim.

Table 4. 2 Descriptive Analysis of the PW from ERA-Interim

	PW_{ARSH} (mm)	PW_{DODM} (mm)	PW_{MTVE} (mm)
μ	26.605	28.279	39.903
σ	5.537	7.123	10.722
max	44.328	44.695	64.482
min	10.684	11.429	17.966
rang	33.644	33.266	46.517

From Table 4.2, the minimum daily average value of PWV for the year 2015 are 10.684mm, 11.429mm and 17.966mm for ARSH, DODM and MTVE respectively. The maximum daily average values of PWV for the year 2015 are 44.328mm, 44.695mm and 64.482mm for ARSH, DODM and MTVE respectively. The station with the minimum daily value of PWV is DODM which falls within the temperate region of the country and the station with the maximum daily value of PWV is MTVE falls within the tropical region of the country where rainfall is high.

4.3 The comparison between Global Reanalysis data and GNSS computed PW for ARSH Cors Station.

The computed values of PW from GNSS signals were analyzed against the data from Global reanalysis models of ERA-Interim. The analysis was based on time series analysis, descriptive statistics and Correlation analysis of the PW values in which both values were decimated to daily data.

4.3.1 Time series analysis of PW of Era-interim and PW computed from GAMIT/GLOBK

The temporal pattern of estimated water vapour from GNSS observation for the study period is compared with reanalysis data models of Era-interim for station ARSH in Figure 4.5.

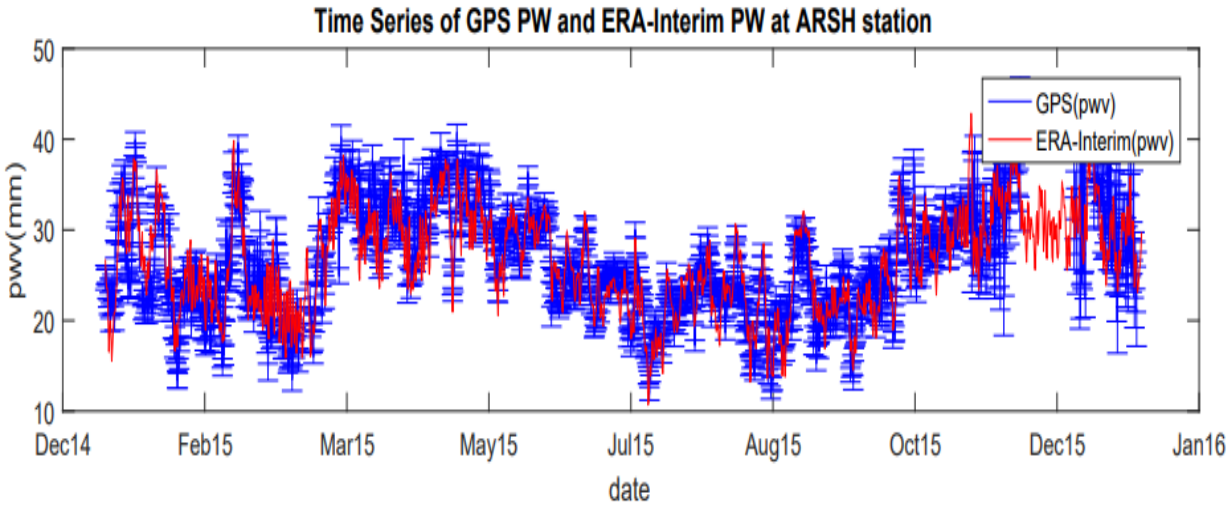

Figure 4. 5 Comparison of PWgamit and PWERA-Interim for ARSH station

From Figure 4.5, both PWs show the trend with closely the same shape with relatively smaller values in dry season and larger values during wet season. The departure between the two

graphs is vivid and different in each season. During the dry season, the values of $PW_{ERA\text{-}Interim}$ are mainly larger than values of PW_{GAMIT} contrary to the wet season in which PW_{GAMIT} has oversampled $PW_{ERA\text{-}Interim}$ in majority. Also, the error bars are visual indicators that represent the uncertainty or variability associated with the computed precipitable water vapour, the length of the error bars indicates the level of higher uncertainty or variability. The longer error bars indicated higher uncertainty, suggesting a wider range of potential values of PWV while shorter suggested greater precision or confidence of the PWV values. It can be observed that for stations with minimal data gap, the temporal characteristics of the PWV estimated from ground-based GNSS stations is the same for the Era-interim PWV.

4.3.2 The Descriptive Analysis of PW of ERA-Interim and PW from GAMIT/GLOBK

The comparison on descriptive statistics of $PW_{ERA\text{-}Interim}$ and PW_{GAMIT} was performed for ARSH station as given in Table 4.3 with their differences.

Table 4. 3 Descriptive Analysis of PWERA-Interim and Computed PW for ARSH Station

	PW_{GAMIT} (mm)	$PW_{ERA\text{-}Interim}$ (mm)	$diff_{ERA\text{-}GAMIT}$ (mm)
μ	26.588	26.605	0.0173
σ	5.868	5.537	-0.330
max	43.810	44.328	2.398
min	11.930	10.684	-1.246
rang	30.000	33.644	3.644

The difference between descriptive statistics of these values showed a mixture of positive and negative differences implying that no value is mainly larger than the other throughout the trend. During the wet season, the maximum value of $PW_{ERAInterim}$ had larger value than PW_{GAMIT} and the minimum value during the dry season had larger value of PW_{GAMIT} than $PW_{ERA\text{-}Interim}$ which support the argument as seen in Figure 4.5 on the trends.

4.3.3 Difference between the PW from GAMIT and PW from reanalysis data Era-interim

Figure 4.6 shows the difference between the computed PW for Cors station ARSH and the IWV from the reanalysis data model of ERA-Interim.

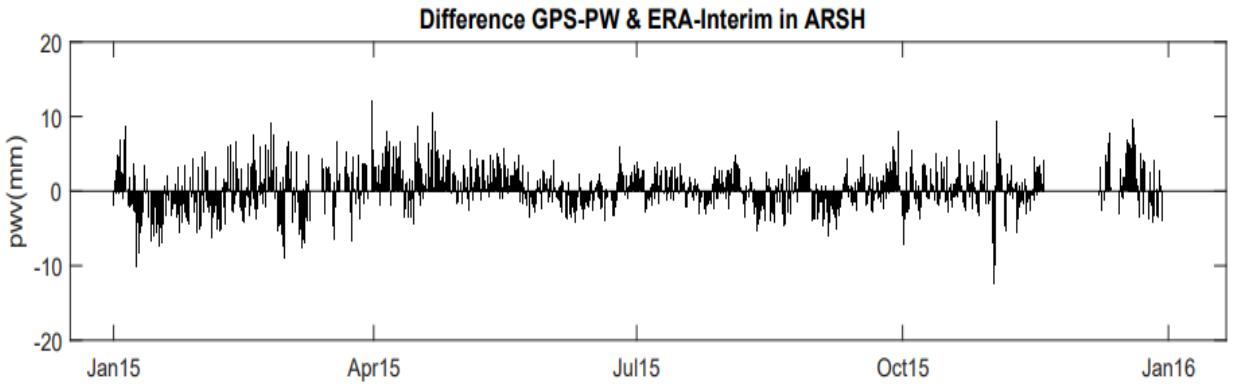

Figure 4. 6 Difference between PWERA-interim and PWgamit for ARSH station

4.3.4 The correlation analysis between the PW computed from GAMIT and PW from reanalysis data Era-interim

The assessment of the relationship between $PW_{ERA\text{-}Interim\ and}$ PW_{GAMIT} was performed by using Pearson correlation coefficient. The correlation between them was positive (strong) with r value of 0.81859. The correlation between values of $PW_{ERA\text{-}Interim\ and}$ PW_{GAMIT} was also depicted using a scatter plot in Figure 4.7 in which the linear-fit was used and linear equation of the best fit line is shown on the graph.

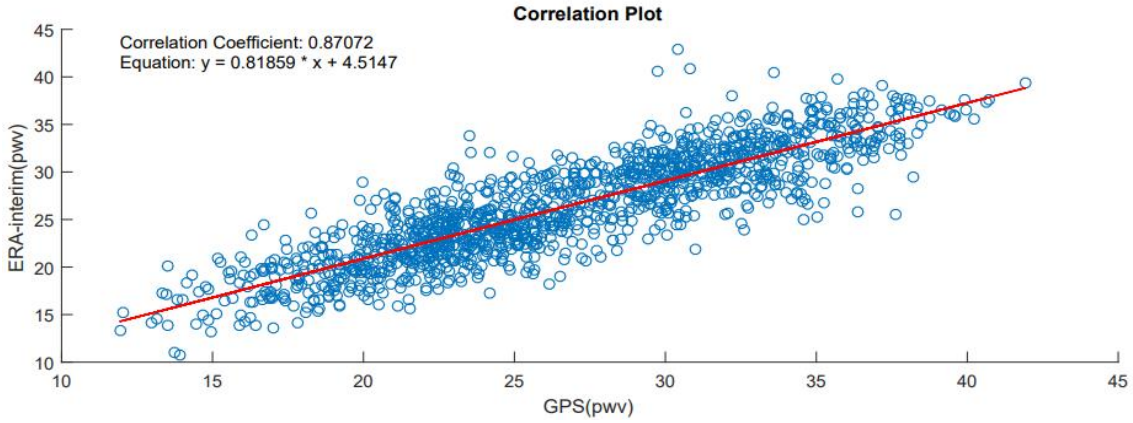

Figure 4. 7 Correlation between the Computed PW and the PWERA-Interim for ARSH

4.4 The comparison between Global Reanalysis data and GNSS computed PW for DODM Cors Station.

The computed vales of PW from GNSS signals were analyzed against the data from Global reanalysis models of ERA-Interim. The analysis was based on time series analysis, descriptive statistics and Correlation analysis of the PW values in which both values were decimated to daily data.

4.4.1 Time series analysis of PW of Era-interim and PW computed from GAMIT/GLOBK

The temporal pattern of estimated water vapour from GNSS observation for the study period is compared with reanalysis data models of Era-interim for station DODM in Figure 4.8.

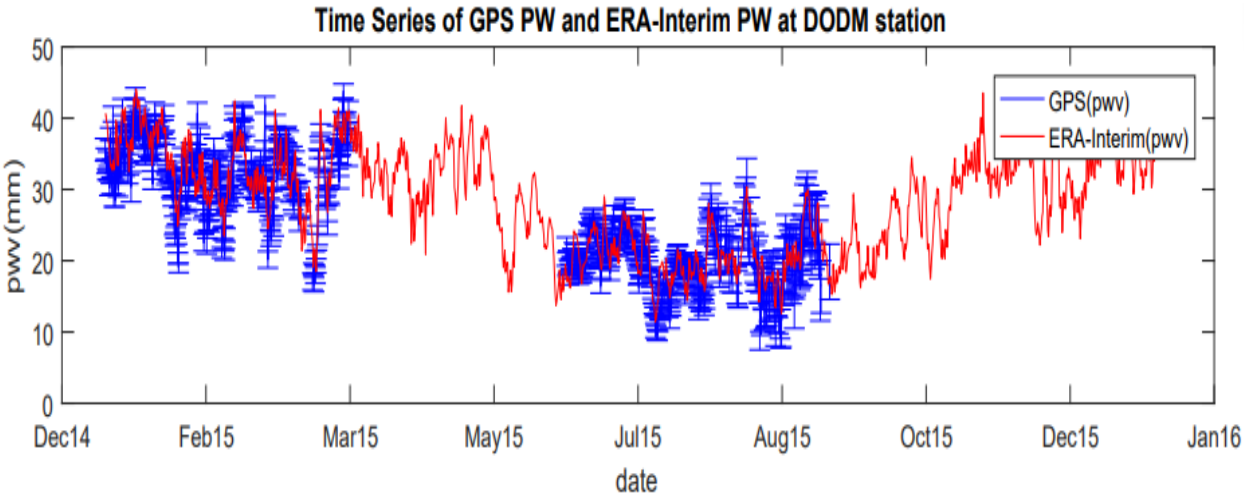

Figure 4. 8 Comparison of PWgamit and PWERA-Interim for DODM station

From Figure 4.8, both PWs show the trend with closely the same shape with relatively smaller values in dry season and larger values during wet season. The departure between the two graphs is vivid and different in each season. During the dry season, the values of $PW_{ERA\text{-}Interim}$ are mainly larger than values of PW_{GAMIT} contrary to the wet season in which PW_{GAMIT} has oversampled $PW_{ERA\text{-}Interim}$ in majority. Also, the error bars are visual indicators that represent the uncertainty or variability associated with the computed precipitable water vapour, the length of the error bars indicates the level of higher uncertainty or variability. The longer error bars indicated higher uncertainty, suggesting a wider range of potential values of PWV while shorter suggested greater precision or confidence of the PWV values. It can be observed that for stations with

minimal data gap, the temporal characteristics of the PWV estimated from ground-based GNSS stations is the same for the Era-interim PWV.

4.4.2 The Descriptive Analysis of PW of ERA-Interim and PW from GAMIT/GLOBK

The comparison on descriptive statistics of $PW_{ERA\text{-}Interim}$ and PW_{GAMIT} was performed for DODM station as given in Table 4.4 with their differences.

Table 4. 4 Descriptive Analysis of PWERA-Interim and Computed PW for DODM Station

	PW_{GAMIT} (mm)	$PW_{ERA\text{-}Interim}$ (mm)	$diff_{ERA\text{-}GAMIT}$ (mm)
μ	26.450	28.279	1.829
σ	7.917	7.123	-0.794
max	43.810	44.695	0.885
min	9.500	11.429	1.929
rang	34.310	33.266	-1.044

The difference between descriptive statistics of these values showed a mixture of positive and negative differences implying that no value is mainly larger than the other throughout the trend. During the wet season, the maximum value of $PW_{ERAInterim}$ had larger value than PW_{GAMIT} and the minimum value during the dry season had larger value of $PW_{ERA\text{-}Interim}$ than PW_{GAMIT} which support the argument as seen in Figure 4.8 on the trends.

4.4.3 Difference between the PW from GAMIT and PW from reanalysis data Era-interim

Figure 4.9 shows the difference between the computed PW for Cors station DODM and the IWV from the reanalysis data model of ERA-Interim.

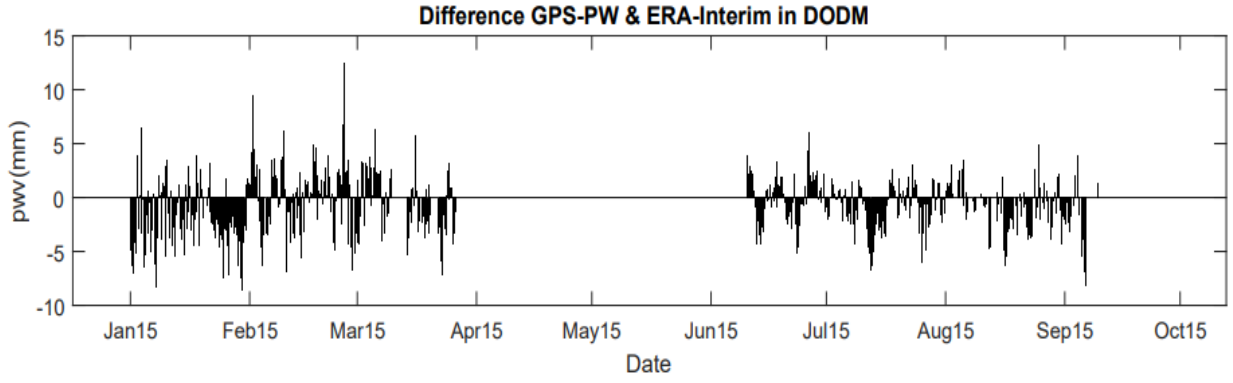

Figure 4. 9 Difference between PWERA-interim and PWgamit for DODM station

4.4.4 The correlation analysis between the PW computed from GAMIT and PW from reanalysis data Era-interim

The assessment of the relationship between $PW_{ERA\text{-}Interim\ and}$ PW_{GAMIT} was performed by using Pearson correlation coefficient. The correlation between them was positive (strong) with r value of 0.92434. The correlation between values of $PW_{ERA\text{-}Interim\ and}$ PW_{GAMIT} was also depicted using a scatter plot in Figure 4.10 in which the linear-fit was used and linear equation of the best fit line is shown on the graph.

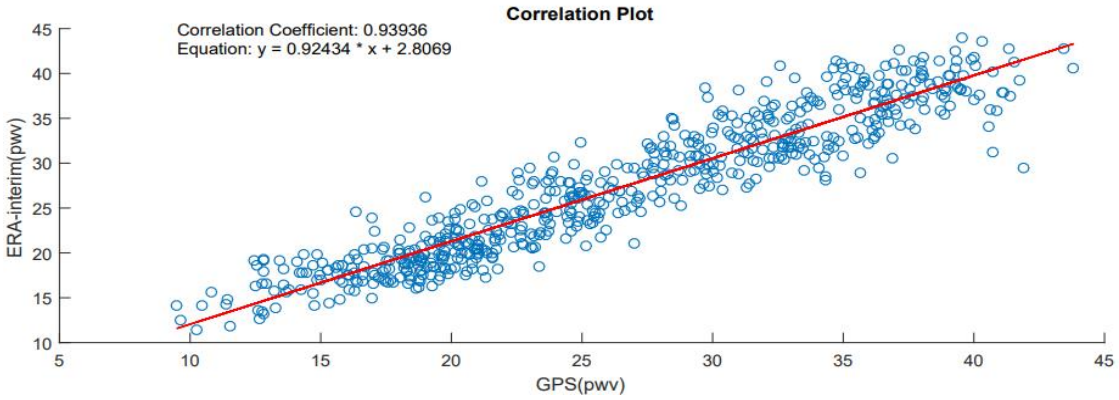

Figure 4. 10 Correlation between the Computed PW and the PWERA-Interim for DODM

4.5 The comparison between Global Reanalysis data and GNSS computed PW for MTVE Cors Station.

The computed values of PW from GNSS signals were analyzed against the data from Global reanalysis models of ERA-Interim. The analysis was based on time series analysis, descriptive statistics and Correlation analysis of the PW values in which both values were decimated to daily data.

4.5.1 Time series analysis of PW of Era-interim and PW computed from GAMIT/GLOBK

The temporal pattern of estimated water vapour from GNSS observation for the study period is compared with reanalysis data models of Era-interim for station MTVE in Figure 4.11.

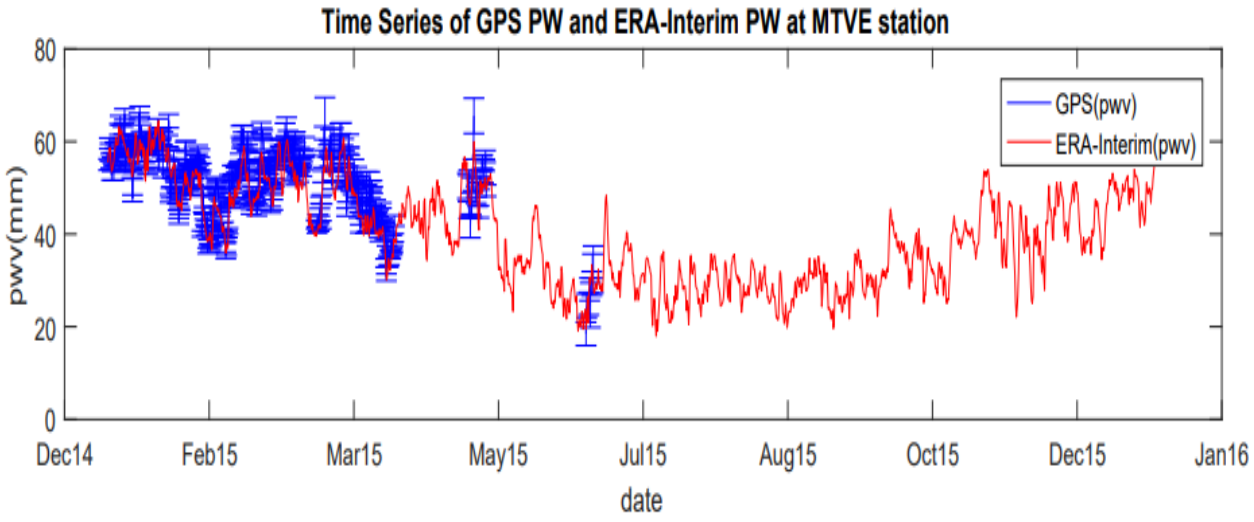

Figure 4. 11 Comparison of PWgamit and PWERA-Interim for MTVE station

From the Figure 4.11, both PWs show the trend with closely the same shape with relatively smaller values in dry season and larger values during wet season. The departure between the two graphs is vivid and different in each season. During the dry season, the values of $PW_{ERA\text{-}Interim}$ are mainly larger than values of PW_{GAMIT} contrary to the wet season in which PW_{GAMIT} has oversampled $PW_{ERA\text{-}Interim}$ in majority. Also, the error bars are visual indicators that represent the uncertainty or variability associated with the computed precipitable water vapour, the length of the error bars indicates the level of higher uncertainty or variability. The longer error bars indicated higher uncertainty, suggesting a wider range of potential values of PWV while shorter suggested greater precision or confidence of the PWV values. It can be observed that for stations with minimal data gap, the temporal characteristics of the PWV estimated from ground-based GNSS stations is the same for the Era-interim PWV.

4.5.2 The Descriptive Analysis of PW of ERA-Interim and PW from GAMIT/GLOBK

The comparison on descriptive statistics of $PW_{ERA\text{-}Interim}$ and PW_{GAMIT} was performed for MTVE station as given in Table 4.5 with their differences.

Table 4. 5 Descriptive Analysis of PWERA-Interim and Computed PW for MTVE Station

	PW_{GAMIT} (mm)	$PW_{ERA\text{-}Interim}$ (mm)	$diff_{ERA\text{-}GAMIT}$ (mm)
μ	51.399	39.903	-11.496
σ	7.957	10.722	2.765
max	66.400	64.482	-1.918
min	18.460	17.966	-0.494
rang	47.940	46.517	-1.423

The difference between descriptive statistics of these values showed a mixture of positive and negative differences implying that no value is mainly larger than the other throughout the trend. During the wet season, the maximum value of PW_{GAMIT} had larger value than $PW_{ERAInterim}$ and the minimum value during the dry season had larger value of PW_{GAMIT} than $PW_{ERA\text{-}Interim}$ which support the argument as seen in Figure 4.11 on the trends.

4.5.3 Difference between the PW from GAMIT and PW from reanalysis data Era-interim

Figure 4.12 shows the difference between the computed PW for Cors station MTVE and the IWV from the reanalysis data model of ERA-Interim.

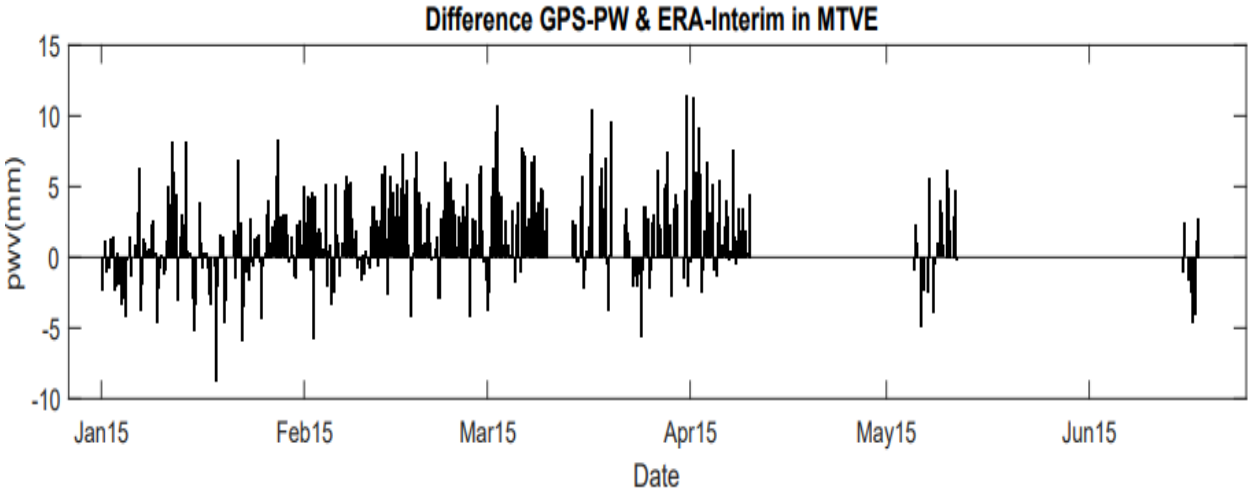

Figure 4. 12 Difference between PWERA-interim and PWgamit for MTVE station

4.5.4 The correlation analysis between the PW computed from GAMIT and PW from reanalysis data Era-interim

The assessment of the relationship between $PW_{ERA\text{-}Interim\ and}$ PW_{GAMIT} was performed by using Pearson correlation coefficient. The correlation between them was positive (strong) with r value of 0.89186. The correlation between values of $PW_{ERA\text{-}Interim\ and}$ PW_{GAMIT} was also depicted using a scatter plot in Figure 4.13 in which the linear-fit was used and linear equation of the best fit line is shown on the graph.

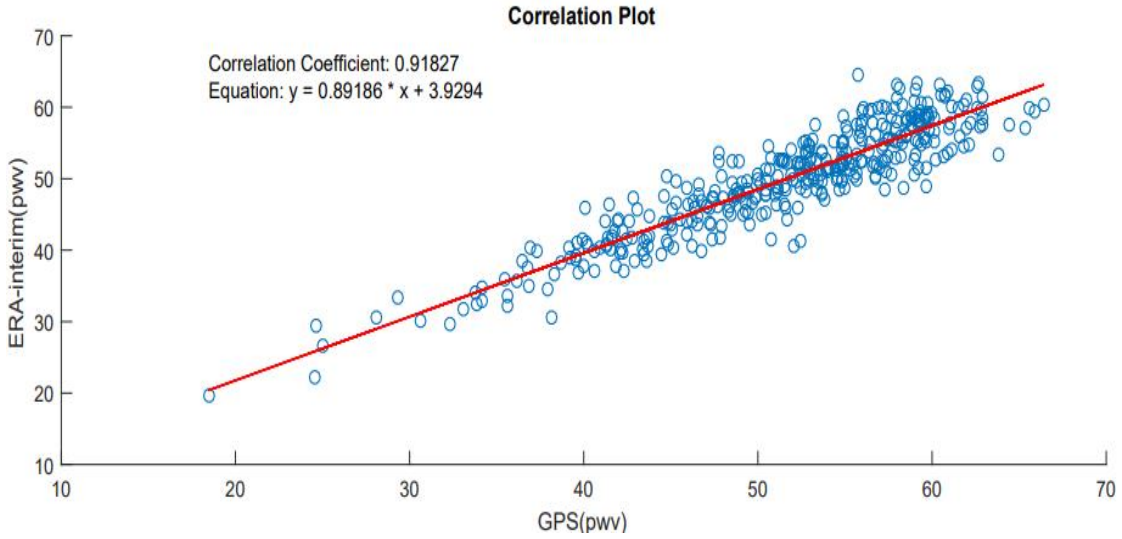

Figure 4. 13 Correlation between the Computed PW and the PWERA-Interim for MTVE

4.7 Summary of the results

The overall relationships between computed GNSS PWs and the data from ERA-Interim are summarized in Table 4.6 showing the Pearson correlation coefficient. Also, Table 4.7 shows the summary on PW values regarding hierarchy of magnitude in descending order from large values to small values for each season.

Table 4. 6 Pearson Correlation Coefficient

No.	GPS	ERA-INTERIM (mm)
1.	DODM	0.92434
2.	MTVE	0.89186
3.	ARSH	0.81859

Table 4. 7 Summary of PW values in wet and dry season

No.		WET (mm)	DRY (mm)
1.	$ARSH_{GAMIT}$	43.810	11.930
2.	$DODM_{GAMIT}$	43.810	9.500
3.	$MTVE_{GAMIT}$	66.400	18.460
4.	$ARSH_{ERA}$	44.328	10.684
5.	$DODM_{ERA}$	44.695	11.429
6.	$MTVE_{ERA}$	64.482	17.966

CHAPTER FIVE

CONCLUSION AND RECOMMENDATION

5.1 CONCLUSION

The aim of this research was to show the comparison between the Precipitable Water Vapour (PWV) computed from GNSS and the Integrated Water Vapour (IWV) from global reanalysis model of ERA-Interim for Numeric Weather Prediction (NWP) in Tanzania. To accomplish this, the precipitable water vapour from three GNSS CORS were determined by using GNSS processing software (GAMIT/GLOBK). A successful determination of PW from ARSH, DODM and MTVE GNSS CORS was achieved which can be used as an input parameter to numeric weather prediction models. Then the computed PW from the processing software were compared with the reanalysis data which were from Era-interim since it is the most effective in weather forecasting. The study conducted a comprehensive analysis of temporal variations and patterns of both datasets facilitating a strong comparison. The results demostrated a similar pattern for an interval of 1 year with great correspondence to Dodoma, Arusha and Mtwara region weather patterns. Also, the results showed a strong positive correlation of 0.92434, 0.89186 and 0.81859 between the PW values derived from GNSS CORS and IWV values from ERA – Interim global model for DODM, MTVE and ARSH station respectively with small difference in individual similar daily values not exceeding 12mm for the both seasons.

The larger differences occurred during dry season for each computed PW than wet season. In both seasons, the values of PW from GAMIT/GLOBK software had smallest difference from IWV from ERA-Interim. The successful descriptive analysis provided valuable insights into the atmospheric moisture content in the region over the study period of 1 year. The ability to assess and compare PW and IWV values is of utmost importance for improving numerical weather prediction models, enhancing weather forecasting accuracy and enabling better preparedness for potential weather – related events in Tanzania. Overall, this research plays a crucial role in advancing the understanding of atmospheric water vapour content and its implications for weather prediction in Tanzania. The positive outcomes achieved in this study shows the importance of GNSS data and global models in enhancing meteorological research and forecasting capabilities. With a more densified network of GNSS stations in Tanzania, the retrieved parameters of Atmospheric water vapour (PW/IWV) will improve NWP in Tanzania.

5.2 RECOMMENDATIONS

Based on the findings of this study, the following recommendations are given:

i) With results from this research showing a great agreement to global reanalysis model data, inclusion of PW computed from GNSS signals by TMA in weather prediction should be taken into consideration.

ii) For further researches, a consideration on determining and analyzing PW from non-meteorological GNSS sites by interpolating ground weather data from nearby weather stations and assessing them if they can be depended on.

REFERENCES

Ahmed , F., Teferle , F. N., Bingley , R. M., & Laur, D. (2015). The Status of GNSS Data Processing Systems to Estimate Integrated Water Vapour for use in Numerical Weather Prediction Models. *International Association of Geodesy Symposia*, 6.

Eresmaa, R., Järvinen, H., Luntama, J. P., & Salonen, K. (2019). *Ground-based GNSS receivers as a meteorological observing system.*

Acheampong, A. A. (2015). *Retrieval of Integrated Water Vapour from GNSS Signals for Numerical Weather Predictions (Issue August). Kwame Nkrumah University of Science and Technology.*

Acheampong, A., Fosu, C., Amekudzi, K. L., & Kaasi, E. (2017). Precipitable Water Comparisons Over Ghana using PPP Techniques and Reanalysis Data. . *South African Journal of Geomatics*, 449–460.

Bevis, M. a. (1994). *GPS Meteorology: Mapping Zenith Wet Delays onto Precipitable Water.*

Bevis, M., Businger, S., Herr, T. A., Rocken, C., Anthes, R. A., & Ware, R. H. (1992). GPS Meteorology' Remote Sensing of Atmospheric Water Vapor by using Global Positioning System. *JOURNAL OF GEOPHYSICAL RESEARCH, 97*, 15,787-15,801.

Borkowf, C. (2002). *Time Series Forecasting by Chris Chateld,Boka Raton,FL:Chapmann and Hall/CRC, 2001, ISBN 1-58488-063-1*.

CIRES. (2020). *Advancing Reanalysis Reanalyses. https://reanalyses.org.*

De haan, S. (2008). *Meteorological applications of a surface network of Global Positioning System receivers.* https://doi.org/ January 2008

Dee, D., Fasullo, J., Shea, D., & Walsh, J. (2020). *Atmospheric Reanalysis: Overview & Comparison Tables. https://doi.org/10.1080/01490419.2013.859642.*

Eresmaa, R. (2022). Ground-based GNSS receivers as a meteorological observing system . *Finish Meteorological Institute*, 7.

Gleisner, H., & Thelji, P. (2016). *Reanalysis data. March 2015.*

Gogtay, N. J., & Thatte , U. M. (2017). *Statistics for Researchers Principles of Correlation Analysis. 65(March), 78–81*.

Guerova, G. (2003). *Application of GPS derived water vapour for Numerical Weather Prediction in Switzerland.* . University of Bern.

Ha, J., Park, K., Kim, K., & Kim, Y. (2010). *Comparison of Atmospheric Water Vapor Profiles Obtained by GPS , MWR , and Radiosonde. 233–241https://doi.org/10.1007/s13143-010-1012-1*.

Haan, S. D. (2011). *Impact of GPS ZTD on rainfall estimates in an hourly update cycle of a numerical weather prediction model.*

Herring, T. A., King, R. W., Floyd, M. A., Mcclusky, S. C., & Sciences, P. (2015). *Gamit Reference Manual GPS Analysis at MIT.*

Hofmann, B., Lichtenegger, H., & Wasle, E. (2008). *GNSS – Global Navigation Satellite Systems GPS, GLONASS, Galileo, and more* . Springer Wien New York.

Hofmann-Wellenhof, B. a. (2001). *GPS. Theory and practise.* New York.

Ise, T. Y. (2013). Weather Forecasting Models, Methods and Applications. *International Journal of Engineering Research & Technology (IJERT)*, 12.

Ishihara, M. (2005). *GPS Meteorology at Japan Meteorological Agency in recent years.*

Leinweber, R. (2010). *Remote Sensing of atmospheric water vapour over land areas using MERIS measurements and application to numerical weather prediction model vaidation.* Freie Universit at Berlin.

Mlawa, A. (2020). *Atmospheric Water Vapour Determination using GNSS Signals for Numeric Weather Prediction in Tanzania.*

Potter, T. D., & Colman, B. R. (2003). *HANDBOOK OF WEATHER, CLIMATE AND WATER. Dynamics, Climate, Physical Meteorology, Weather system and Measurements.*

Pottiaux, E. (2010). *Sounding the Earsth's Atmosphere Water Vapour Using Signals Emitted by Global Navigation Satellite Systems. Université Catholique de Louvain.* Royal Observatory of Belgium.

Schüler, T. (2001). *On Ground-Based GPS Tropospheric Delay Estimation.* Universit¨at der Bundeswehr M¨unchen, Germany.

Shakhashiri. (2010). *Chemical of the week, Water. www.scifun.org.*

Shi, R. &. (2009). *Correlation and regression analysis. Annals of Allergy, Asthma & Immunology.*

Solheim, S., & Ware, R. H. (1999). . *Propagation delays induced in GPS signals by dry air , water vapor , hydrometeors , and other particulates Propagation delays induced in GPS signals by dry air , water vapor , hydrometeors , and other particulates. January.*

Spittlehouse, D. L., Operations, N. R., Development, R., Whitfield, P. H., & Stahl, K. (2008). *Compendium of Forest Hydrology and Geomorphology in British Columbia. January.*

TMA. (2021). *THE TANZANIA METEOROLOGICAL AUTHORITY (METEOROLOGICAL STATIONS)* . Government.

UNAVCO. (2018). *DAI Search.*

Uppala, S. M., Kallberg, P. W., Simmons, A. J., Andrae, U., Betchtold, D. C., Li , X., & Sokka, N. (2005). *The ERA-40 reanalysis. January, 2961–3012.https://doi.org/10.1256/qj.04.176.*

Vedel, H. H.-Y. (2004). *Impact of GPS Zeenith Tropospheric Delay data on precipitation forecasts in Mediterranean France and Spain.*

APPENDICES

APPENDIX I

The following are the processed PW results and IWV from global reanalysis model of ERA-Interim with their differences

MTVE Station

Date	Pwgamit	PW-Era	Difference
mm/dd/yy	mm	mm	mm
1/1/15 6:00 AM	55.03	57.435	-2.405
1/1/15 12:00 PM	59.63	58.456	1.174
1/1/15 6:00 PM	57.68	58.695	-1.015
1/2/15 12:00 AM	55.8	55.994	-0.194
1/2/15 6:00 AM	52.79	53.603	-0.813
1/2/15 12:00 PM	55.09	53.796	1.294
1/2/15 6:00 PM	56.46	54.972	1.488
1/3/15 12:00 AM	53.13	55.496	-2.366
1/3/15 6:00 AM	55.65	57.663	-2.013
1/3/15 12:00 PM	59.21	58.835	0.375
1/3/15 6:00 PM	58.99	60.885	-1.895
1/4/15 12:00 AM	55.96	59.377	-3.417
1/4/15 6:00 AM	56.37	59.314	-2.944
1/4/15 12:00 PM	59.32	59.459	-0.139
1/4/15 6:00 PM	59.12	63.286	-4.166
1/5/15 12:00 AM	62.59	62.857	-0.267
1/6/15 6:00 AM	61.94	60.994	0.946
1/6/15 12:00 PM	62.79	59.577	3.213
1/6/15 6:00 PM	65.88	59.513	6.367
1/7/15 12:00 AM	54.92	58.728	-3.808
1/7/15 6:00 AM	55.99	57.939	-1.949

DODM Station

Pwgamit	PW-Era	Difference
mm	mm	mm
34.99	40.545	-5.555
33.13	39.451	-6.321
32.08	39.134	-7.054
33.99	36.892	-2.902
32.35	36.488	-4.138
30.22	35.400	-5.180
37.74	33.832	3.908
32.38	33.163	-0.783
30.56	33.533	-2.973
32.91	32.693	0.217
40.58	34.050	6.530
29.45	32.749	-3.299
33	33.222	-0.222
28.42	34.972	-6.552
34.36	39.687	-5.327
35.78	39.018	-3.238
31.97	36.976	-5.006
34.1	36.511	-2.411
37.24	40.283	-3.043
41.56	41.235	0.325
34.93	41.137	-6.207

ARSH Station

Pwgamit	PW-Era	Difference
mm	mm	mm
24.800	24.322	0.478
24.950	23.536	1.414
23.170	23.470	-0.300
22.740	20.001	2.739
21.500	16.554	4.946
23.830	19.313	4.517
19.550	20.002	-0.452
23.230	18.516	4.714
21.560	15.567	5.993
24.190	17.217	6.973
21.400	18.822	2.578
22.960	20.714	2.246
19.880	20.820	-0.940
27.870	21.086	6.784
29.430	22.904	6.526
32.610	23.928	8.682
33.880	33.670	0.210
30.860	32.757	-1.897
29.170	31.230	-2.060
36.370	34.491	1.879
33.650	35.665	-2.015

1/7/15 12:00 PM	58.79	57.516	1.274	35.8	39.472	-3.672	33.580	35.405	-1.825
1/7/15 6:00 PM	57.88	56.837	1.043	32.58	40.893	-8.313	33.280	33.249	0.031
1/16/15 6:00 AM	61.13	60.033	1.097	38.73	35.794	2.936	36.950	33.161	3.789
1/16/15 12:00 PM	59.71	60.497	-0.787	37	35.914	1.086	23.980	24.634	-0.654
1/16/15 6:00 PM	58.79	58.467	0.323	35.1	38.091	-2.991	21.490	25.913	-4.423
1/17/15 12:00 AM	59.27	58.911	0.359	36.49	38.057	-1.567	26.090	29.678	-3.588
1/17/15 6:00 AM	60.72	61.509	-0.789	33.28	33.400	-0.120	22.990	30.440	-7.450
1/17/15 12:00 PM	60.4	63.036	-2.636	30.75	35.236	-4.486	24.220	29.162	-4.942
1/17/15 6:00 PM	57.97	61.314	-3.344	36.73	38.834	-2.104	20.680	27.701	-7.021
1/18/15 6:00 AM	62.67	63.338	-0.668	41.38	37.516	3.864	24.850	29.374	-4.524
1/18/15 12:00 PM	55.72	64.482	-8.762	39.47	38.173	1.297	25.660	29.163	-3.503
1/18/15 6:00 PM	58.27	60.329	-2.059	35.08	39.514	-4.434	29.090	29.320	-0.230
1/19/15 6:00 AM	61.48	59.838	1.642	39.07	36.433	2.637	35.340	36.575	-1.235
1/19/15 12:00 PM	61.81	60.292	1.518	38.05	37.285	0.765	32.670	35.963	-3.293
1/19/15 6:00 PM	58.1	62.681	-4.581	37.99	39.941	-1.951	33.250	31.159	2.091
1/20/15 12:00 AM	57.12	60.160	-3.040	38.04	39.832	-1.792	30.290	30.929	-0.639
1/21/15 6:00 AM	57.54	55.705	1.835	38.92	37.997	0.923	30.500	33.899	-3.399
1/21/15 12:00 PM	55.14	56.707	-1.567	41.07	37.917	3.153	29.760	32.219	-2.459

1/21/15 6:00 PM	60.15	58.589	1.561	37.24	38.641	-1.401	31.930	32.007	-0.077
1/22/15 12:00 AM	64.43	57.527	6.903	35.54	37.904	-2.364	31.490	32.979	-1.489
1/22/15 6:00 AM	57.2	54.673	2.527	31.47	33.993	-2.523	26.950	28.668	-1.718
1/22/15 12:00 PM	47.73	53.671	-5.941	32.76	32.744	0.016	22.470	24.185	-1.715
1/22/15 6:00 PM	48.89	52.453	-3.563	32.11	35.136	-3.026	24.550	23.570	0.980
1/23/15 12:00 AM	51.64	52.264	-0.624	31.29	35.006	-3.716	23.870	25.496	-1.626
1/23/15 6:00 AM	52.88	53.919	-1.039	31.92	32.742	-0.822	22.360	25.872	-3.512
1/23/15 12:00 PM	53.01	54.649	-1.639	30.85	32.922	-2.072	21.590	24.625	-3.035
1/23/15 6:00 PM	57.14	54.338	2.802	31.71	34.255	-2.545	30.920	27.595	3.325
1/24/15 12:00 AM	54.89	55.299	-0.409	30.4	35.099	-4.699	23.560	28.306	-4.746
1/24/15 6:00 AM	50.71	51.317	-0.607	29.47	32.068	-2.598	22.360	27.903	-5.543
1/24/15 12:00 PM	51.9	50.560	1.340	28.36	31.894	-3.534	20.930	22.901	-1.971
1/24/15 6:00 PM	48.6	47.105	1.495	30	33.984	-3.984	22.850	22.132	0.718
1/25/15 12:00 AM	47.72	46.053	1.667	24.93	32.350	-7.420	19.010	23.145	-4.135
1/25/15 6:00 AM	45.96	46.354	-0.394	23.02	29.533	-6.513	21.980	23.678	-1.698
1/25/15 12:00 PM	42.84	47.259	-4.419	23.96	26.852	-2.892	16.910	17.389	-0.479
1/25/15 6:00 PM	45.09	45.800	-0.710	30.18	28.437	1.743	20.160	16.617	3.543
1/26/15 12:00 AM	46.34	46.035	0.305	23.77	26.861	-3.091	16.400	19.285	-2.885

1/26/15 6:00 AM	49.71	46.666	3.044	20.36	24.911	-4.551	16.670	19.629	-2.959
1/26/15 12:00 PM	49.14	45.081	4.059	18.99	26.225	-7.235	13.490	17.124	-3.634
1/26/15 6:00 PM	49.41	48.396	1.014	28.26	28.755	-0.495	13.360	17.299	-3.939
1/27/15 12:00 AM	50.17	49.445	0.725	27.77	30.079	-2.309	16.730	19.847	-3.117
1/27/15 6:00 AM	52.95	50.849	2.101	26.72	29.487	-2.767	16.060	20.499	-4.439
1/27/15 12:00 PM	53.91	51.355	2.555	29.9	31.625	-1.725	17.450	20.371	-2.921
1/27/15 6:00 PM	59.07	53.310	5.760	34.85	36.029	-1.179	24.030	22.218	1.812
1/28/15 12:00 AM	58.95	50.672	8.278	33.42	36.727	-3.307	22.310	23.146	-0.836
1/28/15 6:00 AM	55.19	52.265	2.925	32.17	34.917	-2.747	23.020	23.318	-0.298
1/28/15 12:00 PM	54.6	51.717	2.883	32.33	34.595	-2.265	22.160	22.552	-0.392
1/28/15 6:00 PM	53.98	51.007	2.973	33.76	37.296	-3.536	26.140	21.788	4.352
1/29/15 12:00 AM	51.07	49.037	2.033	28.46	34.869	-6.409	20.360	22.763	-2.403
1/29/15 6:00 AM	52.89	49.807	3.083	28.21	30.855	-2.645	22.960	25.713	-2.753
1/29/15 12:00 PM	49.01	47.466	1.544	27.66	31.709	-4.049	23.140	24.633	-1.493
1/29/15 6:00 PM	49.07	49.360	-0.290	29.8	37.313	-7.513	24.820	25.039	-0.219
1/30/15 12:00 AM	52.99	51.551	1.439	29.72	38.413	-8.693	20.860	26.304	-5.444
1/30/15 6:00 AM	53.67	53.517	0.153	31.59	35.737	-4.147	22.190	27.700	-5.510

1/30/15 12:00 PM	51.37	52.696	-1.326	31.75	35.325	-3.575	22.340	22.043	0.297
1/30/15 6:00 PM	51.21	52.653	-1.443	35.38	37.946	-2.566	26.220	23.066	3.154
1/31/15 12:00 AM	55.05	52.706	2.344	33.85	36.929	-3.079	22.690	27.919	-5.229
1/31/15 6:00 AM	56.39	53.757	2.633	32.9	31.727	1.173	24.650	28.879	-4.229
1/31/15 12:00 PM	54.86	53.969	0.891	33.47	31.628	1.842	19.000	23.767	-4.767
1/31/15 6:00 PM	53.06	52.854	0.206	33.86	32.456	1.404	25.650	21.110	4.540
2/1/15 12:00 AM	58.19	53.228	4.962	33.34	32.129	1.211	22.690	23.349	-0.659
2/1/15 6:00 AM	54.08	51.568	2.512	30.04	29.006	1.034	23.370	26.122	-2.752
2/1/15 12:00 PM	54.59	50.216	4.374	33.5	29.215	4.285	21.880	22.974	-1.094
2/1/15 6:00 PM	57.44	53.253	4.187	35.01	30.821	4.189	26.690	21.483	5.207
2/2/15 12:00 AM	51.56	52.553	-0.993	40.7	31.241	9.459	24.730	22.143	2.587
2/2/15 6:00 AM	54.51	49.845	4.665	34.05	29.523	4.527	26.560	23.801	2.759
2/2/15 12:00 PM	40.1	45.933	-5.833	32.65	30.786	1.864	22.300	23.507	-1.207
2/2/15 6:00 PM	49.44	45.150	4.290	36.21	34.867	1.343	25.110	22.268	2.842
2/3/15 12:00 AM	46.53	44.836	1.694	37.19	34.166	3.024	22.180	24.446	-2.266
2/3/15 6:00 AM	45.07	42.977	2.093	30.31	30.643	-0.333	25.550	26.588	-1.038
2/3/15 12:00 PM	43.75	42.022	1.728	33.72	31.009	2.711	21.090	23.889	-2.799
2/3/15 6:00 PM	41.29	40.683	0.607	32.93	35.176	-2.246	20.590	22.597	-2.007
2/4/15 12:00 AM	40.59	39.968	0.622	27.53	32.117	-4.587	21.050	27.275	-6.225
2/4/15 6:00 AM	43.59	38.471	5.119	22.54	28.869	-6.329	21.720	26.754	-5.034
2/4/15 12:00 PM	36.45	38.487	-2.037	25.21	28.661	-3.451	18.600	22.117	-3.517

2/4/15 6:00 PM	39.55	39.106	0.444	31.51	31.648	-0.138	20.240	22.557	-2.317
2/5/15 12:00 AM	39.54	38.619	0.921		29.984	-29.984	22.090	24.727	-2.637
2/5/15 6:00 AM	36.91	40.330	-3.420	24.55	27.834	-3.284	17.830	20.661	-2.831
2/5/15 12:00 PM	37.29	39.835	-2.545	25.16	28.160	-3.000	17.050	18.990	-1.940
2/5/15 6:00 PM	42.29	37.153	5.137	26.33	29.808	-3.478	23.480	20.288	3.192
2/6/15 12:00 AM	38.31	36.660	1.650	27.7	29.408	-1.708	18.420	23.645	-5.225
2/6/15 6:00 AM	42.79	41.690	1.100	24.91	27.358	-2.448	22.350	27.055	-4.705
2/6/15 12:00 PM	45.27	46.575	-1.305	27.33	28.865	-1.535	21.010	24.675	-3.665
2/6/15 6:00 PM	48.95	47.963	0.987	31.66	28.184	3.476	21.930	22.470	-0.540
2/7/15 12:00 AM	47.06	46.211	0.849	30.03	29.882	0.148	17.410	22.810	-5.400
2/7/15 6:00 AM	51.06	46.364	4.696	30.76	28.901	1.859	19.310	24.455	-5.145
2/7/15 12:00 PM	51.57	45.835	5.735	34.26	30.654	3.606	17.350	20.566	-3.216
2/7/15 6:00 PM	50.48	45.348	5.132	36.28	34.243	2.037	20.060	19.762	0.298
2/8/15 12:00 AM	50.24	44.940	5.300	34.35	32.967	1.383	22.730	22.189	0.541
2/8/15 6:00 AM	48.3	45.511	2.789	32.32	30.490	1.830	23.650	21.935	1.715
2/8/15 12:00 PM	45.5	44.251	1.249	29.17	30.115	-0.945	19.100	21.320	-2.220
2/8/15 6:00 PM	44.62	43.940	0.680	33.4	34.047	-0.647	24.410	23.314	1.096
2/9/15 12:00 AM	45.93	43.979	1.951	33.19	33.841	-0.651	22.050	26.617	-4.567
2/9/15 6:00 AM	41.75	42.561	-0.811	33.92	30.443	3.477	26.010	25.502	0.508
2/9/15 12:00 PM	40.22	40.478	-0.258	31.42	27.691	3.729	22.300	21.166	1.134
2/9/15 6:00 PM	39.89	41.499	-1.609	34.3	28.110	6.190	25.650	19.749	5.901
2/18/15 6:00 AM	60.66	53.214	7.446	40.6	36.020	4.580	23.540	20.849	2.691
2/18/15 12:00 PM	57.13	52.546	4.584	36.73	34.675	2.055	28.220	29.182	-0.962

2/18/15 6:00 PM	53.41	49.644	3.766	32.85	34.896	-2.046	34.630	27.147	7.483
2/19/15 12:00 AM	47.45	47.390	0.060	32.73	32.072	0.658	34.380	30.210	4.170
2/19/15 6:00 AM	47.08	46.197	0.883	31.9	31.561	0.339	26.950	29.428	-2.478
2/19/15 12:00 PM	44.87	43.854	1.016	32.17	30.520	1.650	22.310	26.087	-3.777
2/19/15 6:00 PM	48.46	45.066	3.394	32.68	31.798	0.882	28.010	25.253	2.757
2/20/15 12:00 AM	49.3	45.390	3.910	30.96	31.575	-0.615	22.320	24.769	-2.449
2/20/15 6:00 AM	48.8	47.737	1.063	29.83	29.937	-0.107	21.700	23.451	-1.751
2/20/15 12:00 PM	46.73	46.913	-0.183	31.7	30.170	1.530	20.820	20.101	0.719
2/20/15 6:00 PM	47.35	47.348	0.002	34.64	31.815	2.825	27.730	21.731	5.999
2/21/15 12:00 AM	47.99	47.336	0.654	31.33	31.103	0.227	22.030	22.561	-0.531
2/21/15 6:00 AM	49.45	48.038	1.412	29.66	27.657	2.003	23.880	22.663	1.217
2/21/15 12:00 PM	44.6	47.595	-2.995	31.3	27.334	3.966	21.200	21.629	-0.429
2/21/15 6:00 PM	45.92	48.790	-2.870	33.02	31.041	1.979	23.310	22.443	0.867
2/22/15 12:00 AM	50.47	47.773	2.697	31.47	32.692	-1.222	22.220	23.857	-1.637
2/22/15 6:00 AM	52.76	49.490	3.270	29.45	30.786	-1.336	25.330	23.676	1.654
2/22/15 12:00 PM	56.77	50.076	6.694	29.7	29.399	0.301	19.900	20.129	-0.229
2/22/15 6:00 PM	54.88	54.991	-0.111	28.96	33.108	-4.148	27.230	20.954	6.276

2/23/15 12:00 AM	62.91	57.661	5.249	28.13	32.977	-4.847	21.810	23.922	-2.112
2/23/15 6:00 AM	61.96	57.208	4.752	28.12	29.932	-1.812	23.180	23.331	-0.151
2/23/15 12:00 PM	61.55	55.965	5.585	29.5	29.847	-0.347	21.370	21.330	0.040
2/23/15 6:00 PM	59.22	55.136	4.084	33.31	31.824	1.486	28.260	22.818	5.442
2/24/15 12:00 AM	54.94	51.869	3.071	34.43	32.042	2.388	22.650	22.658	-0.008
2/24/15 6:00 AM	53.36	52.690	0.670	32.17	29.549	2.621	25.010	23.187	1.823
2/24/15 12:00 PM	52.66	51.958	0.702	32.51	30.491	2.019	22.160	20.895	1.265
2/24/15 6:00 PM	54.85	52.005	2.845	30.69	33.161	-2.471	31.000	21.842	9.158
2/25/15 12:00 AM	53.98	51.470	2.510	33	31.778	1.222	25.070	22.277	2.793
2/25/15 6:00 AM	55.5	51.868	3.632	35.65	28.932	6.718	23.310	20.478	2.832
2/25/15 12:00 PM	52.27	52.297	-0.027	41.89	29.420	12.470	22.540	19.869	2.671
2/25/15 6:00 PM	54.72	51.892	2.828	32.33	31.779	0.551	26.500	18.996	7.504
2/26/15 12:00 AM	55.54	50.322	5.218	29.49	27.184	2.306	21.550	21.440	0.110
2/26/15 6:00 AM	45.29	49.547	-4.257	28.51	26.036	2.474	23.680	24.746	-1.066
2/26/15 12:00 PM	50.46	49.812	0.648	20.16	24.460	-4.300	25.120	22.396	2.724
2/26/15 6:00 PM	49.28	46.594	2.686	28.79	25.225	3.565	22.830	19.563	3.267
2/27/15 12:00 AM	46.34	46.045	0.295	27.2	26.025	1.175	17.450	21.817	-4.367

2/27/15 6:00 AM	49.87	47.291	2.579	25.33	26.332	-1.002	20.980	26.279	-5.299
2/27/15 12:00 PM	51.13	50.280	0.850	23.12	27.687	-4.567	14.320	19.104	-4.784
2/27/15 6:00 PM	55.66	49.779	5.881	23.9	30.694	-6.794	19.070	17.955	1.115
2/28/15 12:00 AM	56.75	50.270	6.480	31.21	31.232	-0.022	18.710	23.069	-4.359
2/28/15 6:00 AM	54.8	52.855	1.945	27.38	28.508	-1.128	20.220	26.032	-5.812
2/28/15 12:00 PM	54.79	55.091	-0.301	24.67	29.918	-5.248	17.780	20.964	-3.184
2/28/15 6:00 PM	55.89	57.591	-1.701	33.04	36.420	-3.380	22.330	20.459	1.871
3/1/15 12:00 AM	56.08	59.886	-3.806	36.94	41.121	-4.181	18.280	25.645	-7.365
3/1/15 6:00 AM	57.36	59.907	-2.547	39.69	38.040	1.650	19.980	28.940	-8.960
3/1/15 12:00 PM	59.76	59.080	0.680	33.59	37.917	-4.327	20.830	20.675	0.155
3/1/15 6:00 PM	59.65	55.285	4.365	31.29	33.024	-1.734	20.310	18.583	1.727
3/2/15 12:00 AM	57.36	51.089	6.271	36.17	32.778	3.392	25.730	22.377	3.353
3/2/15 6:00 AM	57.28	48.393	8.887	36.38	33.337	3.043	30.010	25.893	4.117
3/2/15 12:00 PM	59.67	48.973	10.697	37.53	34.365	3.165	30.390	24.381	6.009
3/2/15 6:00 PM	56.7	52.151	4.549	33.61	36.283	-2.673	27.360	20.627	6.733
3/3/15 12:00 AM	58.08	55.338	2.742	36.66	37.103	-0.443	25.330	23.631	1.699
3/3/15 6:00 AM	62.22	57.905	4.315	36.23	32.973	3.257	25.990	26.018	-0.028
3/3/15 12:00 PM	59.56	58.737	0.823	34.4	31.472	2.928	22.060	17.583	4.477

3/3/15 6:00 PM	62.61	59.986	2.624	34.61	32.825	1.785	24.840	19.646	5.194
3/4/15 6:00 AM	60.01	59.185	0.825	35.97	32.176	3.794	19.780	22.756	-2.976
3/4/15 12:00 PM	57.34	57.148	0.192	35.53	32.811	2.719	19.180	18.608	0.572
3/4/15 6:00 PM	58.32	54.963	3.357	37.55	38.353	-0.803	16.750	17.339	-0.589
3/5/15 6:00 AM	52.93	54.731	-1.801	35.44	32.660	2.780	20.730	22.955	-2.225
3/5/15 12:00 PM	57.73	55.461	2.269	31.05	30.289	0.761	18.700	17.985	0.715
3/5/15 6:00 PM	59.51	55.604	3.906	36.9	30.527	6.373	21.120	15.870	5.250
3/6/15 12:00 AM	52.78	53.865	-1.085	32.73	30.374	2.356	20.080	20.071	0.009
3/6/15 6:00 AM	59.17	51.403	7.767	30.97	28.821	2.149	21.680	23.250	-1.570
3/6/15 12:00 PM	60.18	52.676	7.504	29.32	29.135	0.185	15.180	20.919	-5.739
3/6/15 6:00 PM	60.9	53.717	7.183	33.2	31.005	2.195	15.580	18.754	-3.174
3/7/15 12:00 AM	51.99	49.849	2.141	34.85	32.386	2.464	15.960	21.012	-5.052
3/7/15 6:00 AM	53.23	50.536	2.694	28.17	31.256	-3.086	16.710	24.390	-7.680
3/7/15 12:00 PM	53.9	52.607	1.293	27.61	31.660	-4.050	19.700	21.011	-1.311
3/7/15 6:00 PM	53.84	47.051	6.789	33.68	34.366	-0.686	17.390	17.067	0.323
3/8/15 12:00 AM	52.47	48.825	3.645	32.1	35.400	-3.300	13.500	20.098	-6.598
3/8/15 6:00 AM	57.69	50.573	7.117	29.27	32.262	-2.992	16.310	23.331	-7.021
3/8/15 12:00 PM	54.42	51.296	3.124	30.27	29.738	0.532	19.380	19.319	0.061
3/8/15 6:00 PM	55.26	51.308	3.952	29.71	31.436	-1.726	18.860	17.468	1.392
3/9/15 12:00 AM	53.67	49.757	3.913	29.34	30.867	-1.527	16.910	20.477	-3.567
3/9/15 6:00 AM	54.79	49.903	4.887	25.02	26.491	-1.471	17.980	21.964	-3.984

3/9/15 12:00 PM	57.3	52.558	4.742	26.92	25.192	1.728	17.420	16.434	0.986
3/9/15 6:00 PM	57.42	55.488	1.932	29.84	27.422	2.418	22.460	17.603	4.857
3/10/15 12:00 AM	59.05	55.553	3.497	27.24	24.646	2.594	20.960	21.043	-0.083
3/14/15 6:00 AM	40.9	40.269	0.631	17.07	22.434	-5.364	15.630	19.541	-3.911
3/14/15 12:00 PM	43.49	41.164	2.326	18.79	19.116	-0.326	22.820	18.567	4.253
3/14/15 6:00 PM	41.4	41.769	-0.369	16.66	20.417	-3.757	20.530	16.038	4.492
3/15/15 12:00 AM	41.59	41.949	-0.359	20.37	21.653	-1.283	17.310	16.894	0.416
3/15/15 6:00 AM	44.76	41.229	3.531	17.96	20.354	-2.394	20.030	16.973	3.057
3/15/15 12:00 PM	47.35	41.591	5.759	19.29	18.502	0.788	18.040	19.579	-1.539
3/15/15 6:00 PM	42.03	44.211	-2.181	22.64	21.729	0.911	16.020	19.140	-3.120
3/16/15 12:00 AM	47.5	48.359	-0.859	23.58	24.387	-0.807	21.700	18.572	3.128
3/16/15 6:00 AM	52.44	51.957	0.483	34.3	28.493	5.807	19.710	19.762	-0.052
3/16/15 12:00 PM	55.64	53.455	2.185	33.55	32.342	1.208	25.340	22.441	2.899
3/16/15 6:00 PM	61.83	54.459	7.371	36.43	35.748	0.682	25.100	23.316	1.784
3/17/15 12:00 AM	63.82	53.293	10.527	37.96	41.177	-3.217	27.110	23.895	3.215
3/18/15 12:00 PM	58.99	52.658	6.332	31.01	32.725	-1.715	24.880	29.506	-4.626
3/18/15 6:00 PM	55.92	52.505	3.415	28.12	31.871	-3.751	20.430	26.998	-6.568
3/19/15 12:00 AM	61.12	54.022	7.098	28.47	30.981	-2.511	29.690	28.508	1.182

3/19/15 6:00 AM	57.15	57.581	-0.431	28.82	28.077	0.743	26.210	28.441	-2.231
3/19/15 12:00 PM	50.62	54.422	-3.802	24.59	26.730	-2.140	26.060	26.989	-0.929
3/19/15 6:00 PM	52.29	52.186	0.104	31.57	30.293	1.277	22.140	21.903	0.237
3/20/15 12:00 AM	58.36	48.795	9.565	29.08	32.370	-3.290	28.410	21.674	6.736
3/22/15 12:00 AM	58.23	55.896	2.334	29.16	30.847	-1.687	25.370	23.904	1.466
3/22/15 6:00 AM	61.08	57.676	3.404	35.82	39.095	-3.275	30.440	28.124	2.316
3/22/15 12:00 PM	59.2	57.452	1.748	35.94	38.659	-2.719	30.930	30.931	-0.001
3/22/15 6:00 PM	59.17	57.987	1.183	38.03	40.366	-2.336	31.020	27.812	3.208